INVESTIGATING THE ROLE OF *MLLT11* IN SUBVENTRICULAR ZONE NEUROGENESIS AND DEVELOPMENT OF THE OLFACTORY BULB

by

Mohsen Heidari

Submitted in partial fulfillment of the requirements
for the degree of Masters of Science

Dalhousie University
Halifax, Nova Scotia
August 2022

DEDICATION

To my mother, Elaheh Soleimannejad

This thesis and all my accomplishments would not have been possible without you. This thesis is dedicated to you and I hope it brings you joy to see your son succeed in your footsteps.

To my father, Parviz Heidari

Thank you for always making time to lend a helping hand. You've taught me to keep a level head while solving problems and be curious of my surroundings.

Table of Contents

LIST OF TABLES v
LIST OF FIGURES vi
Abstract ix
LIST OF ABBREVIATIONS USED x
Acknowledgements xiii
CHAPTER 1 INTRODUCTION 1
1.1. *Mllt11* 4
1.2. Organization of the Olfactory Bulb 7
1.3. Origin of the Stem Cell Pool 10
1.4. Formation of the Cortex 11
1.5. Ventricular Zone 12
1.6. Stem Cell Niche of the VZ/SVZ 14
1.7. Migration along the RMS 15
1.8. Formation of the Olfactory Bulb (OB) 17
1.9. Histology of the Olfactory Bulb 18
1.10. Hypothesis and Objectives 20
CHAPTER 2 MATERIAL AND METHODS 23
2.1. Animals 23
2.2. EdU (5-ethynyl-2′-deoxyuridine) Labeling 26
2.3. Cell Culture 26
Neurosphere Assay 26
Passaging and Secondary Cultures 28
Differentiation Assay 28
2.4. Immunohistochemistry 29
2.5. Sampling Methodology 32
2.6. Statistical Methods 33
CHAPTER 3 RESULTS 35
3.1. Expression pattern of *Mllt11* and its knockout using $Emx1^{IRESCre}$ 35
3.2. *Mllt11* knockout results in a drift of NSCs away from the SVZ region 42
3.2.1. EdU profiling of migrating neuroblasts 45
3.3. *Mllt11* loss results in a deficit in NSCs' ability to self-renew 48

3.4. *Mllt11* loss results in a deficit in NSC differentiation..... 53
3.5. *Mllt11* is not required for migration of neuroblasts along the RMS 56
Number of EdU labeled cells was not significantly different 56
3.6. *Mllt11* conditional knockout affects cell packing and cell fate in the Olfactory bulb 60
3.7. *Mllt11*cKO does not present with sex differences in the postnatal brain..... 66
CHAPTER 4 DISCUSSION..... 67
4.1. Summary of Key Findings 67
4.2. *Mllt11* Expression in the SVZ Neurogenic Niche and OB 69
4.3. Misplacement of NSCs Alters their Self-renewal Capacity..... 71
4.4. Role of *Mllt11* in Migration along the RMS..... 72
4. 5. Loss of *Mllt11* resulted in fewer differentiated neurons *in vitro* and *in vivo*..... 76
4. 6. Limitations 78
4. 7. Future Direction 79
Appendix I 81
REFERENCES 82

LIST OF TABLES

Figure #	**Figure Label**	**Page #**
Table 1	Primary Antibodies Used	30-31
Table 2	Secondary Antibodies Used	31-32
Table 3	Experimental mean and P values calculated for each sexes and group data	81

LIST OF FIGURES

Figure #	Figure Label	Page #
Figure 1.1	Organization of the Ventriculo-Olfactory Neurogenic System (VONS)	3
Figure 1.2	Organization of the Olfactory Bulb (OB)	9
Figure 2.1	*Emx1*^{IresCre} is Activated in the Pallial Cortex	25
Figure 2.2	Selection of counting frames along the VONS	34
Figure 3.1	*Mllt11* expression in the ventricular neurogenic niche	38
Figure 3.2	*Mllt11* expression in the Ventriculo-Olfactory Neurogenic System (VONS)	39
Figure 3.3	Orthogonal view of *Mllt11* expression in the VONS	40
Figure 3.4	*Mllt11* expression levels using qPCR	41
Figure 3.5	Thickness of the GFAP band at the SVZ	43
Figure 3.6	Distribution of Sox2+GFAP+ cells in the SVZ	44

Figure #	Figure Label	Page #
Figure 3.7	Loss of *Mllt11* results in accumulation of EdU+ cells at the junction of the SVZ and RMS (P10)	46
Figure 3.8	Accumulation of new born cells at the SVZ persists into adulthood (P30)	47
Figure 3.9	Primary Proliferation Assay at P10	50
Figure 3.10	Secondary Proliferation Assay	51
Figure 3.11	Size Exclusion of Neurospheres	52
Figure 3.12	Neuronal Differentiation Assay	55
Figure 3.13	Average directionality and thickness of Nestin filaments	58
Figure 3.14	Average directionality and thickness of DCX filaments	59
Figure 3.15	Loss of *Mllt11* results in reduced cell density in the MCL	62
Figure 3.16	Loss of *Mllt11* results in increased Tbr2+ cell count and ratio in the MCL at P10	63

Figure #	**Figure Label**	**Page #**
Figure 3.17	Loss of *Mllt11* results in reduced CR+ cell count in the MCL at P30	64
Figure 3.18	Parvalbumin expressing interneurons were not affected by *Mllt11* cKO	65
Figure 4.1	Summary figure	70

Abstract

Neurogenesis is the process of generating new neurons in developing and adult brains. This process imparts plasticity to the mammalian brain by allowing novel connections to form and replacing damaged neurons. In later stages of development, only a handful of neurogenic niches remain active including the sub-ventricular zone and dentate gyrus of the hippocampus. Neurogenic niches are under strict genetic and environmental control to ensure the maintenance of the stem cell pool and identity. While many genetic regulators of ongoing neurogenesis in the adult mammalian brain have been identified, we still have an incomplete picture of the genetic processes that regulate the integration of newborn cells into existing neural circuits. To that end, my thesis work has focused on the function of a novel gene called *Mllt11* in postnatal neurogenesis. It encodes a 90 amino acid protein recently implicated in the maturation of neuronal precursors and transition to post-mitotic neurons. The role *Mllt11* in the regulation of neurogenesis from the subventricular (SVZ) regions abutting the mouse olfactory bulb was explored using conditional loss-of-function mutagenesis to excise the *Mllt11* gene within the precursors that contribute to SVZ neurogenesis. Given that recent work from the lab revealed that *Mllt11* interacts with stabilized microtubules, I hypothesized that it is required to maintain the appropriate connections between precursor cells and their niche environment surrounding the SVZ. Firstly, I explored the activity of the *Mllt11* locus during perinatal development, to determine if it is expressed in neural precursors within the SVZ niche. Secondly, I determined whether *Mllt11* loss impacted the mobilization of newborn neurons from the SVZ niche. Thirdly, I examined whether *Mllt11* loss affected both the proliferation and differentiation of neuronal precursors in the perinatal brain. Lastly, I looked at whether *Mllt11* function was required to replenish the olfactory bulb with newborn neurons. My thesis study has revealed that *Mllt11* is expressed in the neurogenic niche and that it regulates the mobilization of newborn neurons to joining the rostral migratory stream supplying interneurons to the olfactory bulb. Using primary cell culture assays, I also discovered that *Mllt11* is required for the self-renewal of neonatal SVZ neural stem cells, likely reflecting a role of *Mllt11* in tethering neural progenitors to the SVZ niche.

LIST OF ABBREVIATIONS USED

ALS	Amyotrophic Lateral Sclerosis
BMP	Bone Morphogenic Protein
cKO	Conditional Knockout
CNS	Central Nervous System
CR	Calretinin
CSF	Cerebrospinal Fluid
CXCL-13	Chemokine (C-X-C motif) Ligand 1
DCX	Doublecortin
DMSO	Dimethyl Sulfoxide
DRG	Dorsal Root Ganglion
ECM	Extra-Cellular Matrix
EdU	5-Ethynyl-2'-Deoxyuridine
EGF	Epithelial Growth Factor
Emx1	Homeobox Protein Emx1
EPL	External Plexiform Layer
ET	External Tufted Cell
FGF	Fibroblast Growth Factor
GAD	Glutamic Acid Decarboxylase
GCL	Granule Cell Layer

GL	Glomerular Layer
HEK	Human Embryonic Kidney Cells
IPC	Intermediate Progenitor Cell
IRES	Internal Ribosome Entry Site
JG	Juxtaglomerular Cell
LoxP	Locus of X-Over P1
LV	Lateral Ventricle
LVCP	Lateral Ventricle Choroid Plexus
MCL	Mitral Cell Layer
Mllt11/Af1q	Myeloid/Lymphoid or Mixed-Lineage Leukemia; Translocated to Chromosome 11/All1 Fused Gene from Chromosome 1q
mRNA	Messenger Ribonucleic Acid
NPC	Neural Progenitor Cell
NSC	Neural Stem Cell
OB	Olfactory Bulb
OE	Olfactory Epithelium
OSN	Olfactory Sensory Neuron
PBS	Phosphate Buffered Saline
PBT	Phosphate Buffered Tween
PFA	Paraformaldehyde
PG	Paraglomerular Cell

PV	Parvalbumin
q-PCR	Quantitative Polymerase Chain Reaction
Rbp4	Retinol Binding Protein 4
REST	Repressor Element 1 Silencing Transcription Factor
RGC	Radial Glial Cell
RMS	Rostral Migratory Stream
ROI	Region of Interest
SOD1	Superoxide Dismutase 1
Sox2	Sex Determining Region Y-Box 2
sSA	Superficial Short Axon Cell
SVZ	Sub-Ventricular Zone
TGF	Transforming Growth Factor
TH	Tyrosine Hydroxylase
TKI	Tyrosine Kinase Inhibitor
Tubb3	Tubulin Beta 3
VEGF-A	Vascular endothelial growth factor A
VONS	Ventriculo-Olfactory Neurogenic System

Acknowledgements

Dear Dr. Angelo Iulianella, thank you for this unique opportunity to contribute to your research and your unwavering support. You have shaped my future for the better and instilled me with scientific curiosity. I will forever be in awe of your knowledge and achievements. It was an honour to be in your lab and learn from you.

Thank you to my committee members, Dr. Ying Zhang and Dr. Victor Rafuse for your guidance and compassion throughout this journey. Your insight into my work propelled me to reach greater heights.

Dear Danielle Stanton-Turcotte, I can't thank you enough for your help in and out of the lab. You truly are an encyclopaedia of information. Your presence in the lab made graduate life much less intimidating. Your future shines bright like your personality. It was a pleasure to spend graduate school with you. Please remember to send me pictures of your cute cat.

Dear Marley Blommers, you are a true friend. I could always rely on you for scientific advice and good laughs. I know you will succeed anywhere you are because of your diligent and dependable personality. Your friendship was a source of motivation!

Dear Karolynn Hsu, thank you for teaching me so much about cell cultures and sharing your expertise. Your book recommendations are top tier and your taste in movies is immaculate. I wish you the best life has to offer.

Dear Emily Witt, thank you for always reaching out a helping hand and bringing everyone together.

Thank you to all my friends in the department for making graduate life such an enjoyable experience. Even though the pandemic stole a lot of opportunities to socialize we did find our own ways of remaining connected.

Finally, thank you to DMRF and CIHR for providing funding for this research. You made this possible and I hope the results from this thesis contribute to enhancing our understanding of developmental neurobiology.

CHAPTER 1 INTRODUCTION

The olfactory system is a highly complex network of neurons capable of sensing more than 1,000 different odorant molecules (Bushdid et al., 2014). This complex network is reliant on a constant supply of new-born neurons throughout development into adulthood due to aging and formation of novel networks. These new-born neurons come from a few neurogenic niches that remain active at later stages of development. Neurogenic niches are pools of undifferentiated neural stem (NSC) and progenitor (NPC) cells that are proliferative and can give rise to new neurons. Defects in these neurogenic niches result in lifelong discrepancies in cognition, memory, and olfaction (Balu and Lucki, 2009; Bond et al., 2015; Derkach et al., 2021). A variety of molecular controls are in place to regulate and prevent the depletion of NSC population. Among the genes of interest, *Mllt11* encodes for a tubulin interacting protein that has been implicated in the maturation of neuronal precursors and transition to post-mitotic neurons (Stanton-Turcotte et al. 2022). Not surprising is the association found between *Mllt11* gene and neurodevelopmental disorders such as schizophrenia and autism spectrum disorder in genome-wide association studies (Brzustowicz et al., 2002; Su et al., 2017). Neural development requires the appropriate generation of neurons and connections at specific times. Disruptions to cell morphology can alter the connections and chemical cues cells receive and ultimately affect their identity (Habela et al. 2020). The olfactory network consists of a large variety of neurons which require timely generation and maintenance in

order to function (Kim, Jae Yeon et al. 2020; Kao and Lee, 2010; Osterhout et al., 2014).

The main source of interneurons in the olfactory bulb is the sub-ventricular zone (SVZ) of the lateral ventricles (LV). These cells migrate to their destination in the olfactory bulb (OB) via a glial bridge called the rostral migratory stream (RMS) (Figure 1.1). The SVZ remains neurogenic even in adulthood. The interneurons supplied by the SVZ to OB in adulthood allow for olfactory memory (Derkach et al., 2021). The ventriculo-olfactory neurogenic system (VONS) has been studied in-depth to better understand adult neurogenesis to promote brain repair. In this study we examined the role of *Mllt11* in proliferation, differentiation, and migration of ventricular zone precursor cells. Cells receive a wide range of chemical and physical cues to decide their fate and migration. Many of these cues rely on the morphology of the cells and the contacts they make with adjacent cells, blood vessels, and scaffolding proteins. The exact role of Mllt11 intracellularly is unknown, however, by interacting with stabilized microtubules that form the cytoskeleton we hypothesized that Mllt11 is critical to the proper development of neurons and their appropriate migration.

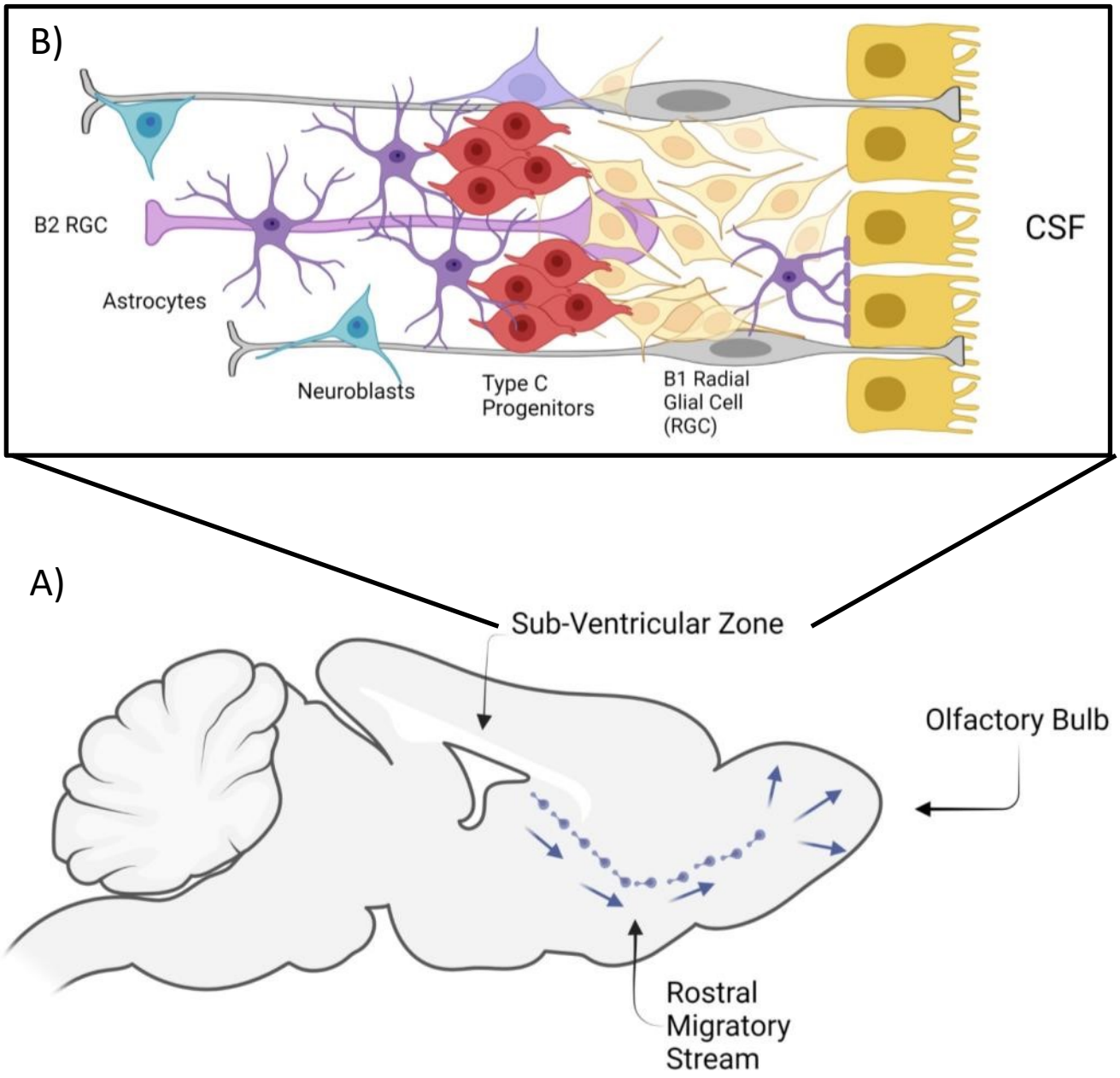

Figure 1.1) Organization of the Ventriculo-Olfactory Neurogenic System (VONS) in Adult Mouse Brain

Neuroblasts are generated from the dorsal horn of the lateral ventricles and migrate to the OB via a glial bridge called the rostral migratory stream (RMS). These cells form chains with the cells at the tip being specialized for sensing chemical cues. A) Sagittal view of the VONS showing the path neuroblasts take to the OB. B) A magnified image of the SVZ showing the organization of the neurogenic niche.

1.1. *Mllt11*

Myeloid/lymphoid or mixed-lineage leukemia; translocated to chromosome 11 or ALL1 fused from chromosome 1q (*Mllt11*/AF1q) encodes for a 90 amino acid protein that is a vertebrate-specific and contains a nuclear export sequence (Tse et al., 1995). *Mllt11* interacts with stabilized microtubules, namely, acetylated- α- tubulin. Our lab has demonstrated that *Mllt11* expression is exclusive to the central and peripheral nervous systems and co-incidents the onset of maturation in neuroblasts. In the peripheral nervous system, *Mllt11* is first detected on E10.5 in the ventral horn and the dorsal root ganglion (DRG) (Yamada et al., 2014). *Mllt11* expression in the cortex is restricted to migrating and nature neurons and has been shown to play a role in migration and cell identity (Stanton-Turcotte et al. 2022). Furthermore, *Mllt11* expression is upregulated in differentiated cortical neurons and serves a role in promoting a neural transcriptional identity for these cells. For example, expression of *Mllt11* in HEK cells has been shown to trigger expression of *Tubb3* a β3-subunit of Tubulin specific to neurons (Lin et al., 2004). The gene is initially expressed on embryonic day (E) 11.5 in the marginal zone of the cortex. Cells in this region constitute the earliest mature neurons as demonstrated by the expression of neuron specific β3-tubulin marker, Tubb3, and absence of the neural progenitor marker, Sox-2. Recent work from our lab has demonstrated expression of *Mllt11* in the mouse hippocampal neural progenitors and proposed that *Mllt11* is important to the maintenance of NSCs.

Despite these findings, the best understood function of the gene is its association with leukemia and hematopoietic cancers. Translocation, duplication and gain of function mutations of *Mllt11* in myeloid tissue result in malignancies and treatment resistance in leukemia patients (Tiberio et al., 2017; Li et al., 2018). These malignancies are a result of the translocation of *Mllt11* to the Trithorax locus (Le Baccon et al., 2001). The aberrant activation promotes cell survival in tumours and removes cell cycle barriers to rapid division. Tyrosine kinase inhibitors (TKI) block the intrinsic cell survival signaling in tumour cells and allow for better treatment efficacy. Leukemia patients with gain of function mutations in *Mllt11* display worse prognosis with TKI treatment. The aberrant activation of *Mllt11* in myeloid tissue promotes survival and presents reserve signaling during TKI treatment, which may contribute to higher rates of cancer metastasis and motility (Chang et al., 2008; Park et al., 2015).

Mllt11 has been implicated in neuronal differentiation and projection of axonal/ dendritic projections due to its downregulation in a sporadic non-SOD1 ALS mutation (Lederer et al., 2007). Lederer and colleagues used whole-genome expression profiling to identify de-regulated genes and interpreted the role of these genes. *Mllt11* was reported to be responsible for dendritic maintenance and its depletion was linked to neuronal loss in this non-SOD1 ALS mutant. Recent studies have also shown a negative correlation between *Mllt11* and the Repressor Element 1 Silencing Transcription Factor (REST). REST is highly expressed in embryonic stem cells, and its expression tapers in progenitors for migration and differentiation to occur. REST overexpression results in

axonal guidance errors and delayed neuronal differentiation (Mandel et al., 2011; Mozzi et al., 2017). Hu and colleagues (2015) reported a down-regulatory effect of the REST transcription factor on *Mllt11* by interacting with a neuron-restrictive silencer element at −383 to −363 bp of human AF1q promoter. Therefore, the negative correlation in expression of *Mllt11* and *REST* could serve as a control mechanism for neuronal differentiation to take place. Additionally, REST has been shown to regulate adult neurogenesis by halting the neurogenic program in quiescent stem cells (Gao *et al.* 2011). Gao and colleagues elaborate on exhaustion of the NSCs and loss of neurogenic capacity in the absence of REST.

Considering its function in disease and its interaction with stabilized microtubules, we hypothesized the role of *Mllt11* under physiological conditions is to define cell morphology, regulate arborization, and migration to the appropriate cortical structure. Our lab has been able to conditionally remove *Mllt11* from progenitors that give rise to neurons in the upper cortical layers using a $Cux2^{iresCre}$ mouse model (Stanton-Turcotte et al., 2022). Stanton-Turcotte and colleagues (2022) showed aberrant morphology of upper layer neurons, a loss of cell transcriptional identity, and reduced white matter tracks of the corpus callosum. Undoubtedly, *Mllt11* has a crucial role in neurodevelopment at the embryonic stages; however, very little is known about the role of *Mllt11* in the stem and progenitor cell pools of the SVZ. Previous lab members have explored the effect of *Mllt11* knockout on hippocampal circuitry and reported a shift in the proliferation of these cells early in development and tapering at later stages. It is

crucial to examine the proliferative and cell identity effects of *Mllt11* knockout in the subventricular zone progenitor pool as they contribute to not only cortical development but also the maintenance of neurogenesis in adulthood. Finally, looking at the olfactory bulb we may be able to assess network integration and observe whether *Mllt11* knockout results in heterotopia of affected migrating neurons.

1.2. Organization of the Olfactory Bulb

Olfaction is a complex process capable of detecting more than 1,000 different odors in humans (Bushdid et al., 2014). This is remarkable when considering the diverse number of receptors that must exist in order to detect these odors. Olfactory sensory neurons (OSNs) line the olfactory epithelium (OE) and express a single type of odorant receptor (Figure 1.2). OSNs detect molecules in the air and relay this information to the OB through projections that arrive at spherical junctions called glomeruli. These structures receive input from a single type of OSN and modulate the transmission of information (Lodovichi and Belluscio, 2012). A glomerulus is therefore divided into two halves with one receiving input from OSNs and the other containing processes from mitral and tufted cells. They receive regulatory input from juxtaglomerular cells consisting of periglomerular (PG) interneurons, superficial short-axon cells (sSA), and external tufted cells (ET) (Figure 1.2). PG cells rarely interact with multiple glomeruli and their axons terminate in the interglomerular layer. These cells express a combination of Gad65/67 and/or TH or Calbindin/ Calretinin. PG interneurons are classified into two

categories: Type-I PG cells extend their dendrites to both halves of the glomerulus interacting with the ONs and the mitral/ tufted cells. While Type-II PG cells only extend dendrites to the non-olfactory neuron half of the glomerulus. Superficial short-axon cells (sSA) are few and extend their axons to 1-2 glomeruli while their dendrites avoid contact. Finally, ET cells are mainly glutamatergic with few GABAergic neurons that receive input from OSNs. These cells synapse onto other juxtaglomerular cells and other projection neurons in the same glomerulus. They are classified into two types: with and without secondary (basal) dendrites (Wilson and Mainen, 2006; Sakano, 2010; Mori and Sakano, 2011; Lodovichi and Belluscio, 2012).

The sense of smell results from specific spatial and temporal patterns of activation in glomeruli nodes. These patterns are largely generated through horizontal inhibition of juxtaglomerular cells. PG cells can receive information from OSNs, ET, and sSA cells and modulate the activity of mitral cells and tufted cells. On the other hand, ET cells receive input from other ET cells and OSNs and synapses onto PG and sSA cells. The network created through the cross talk between juxtaglomerular cells creates a specific pattern of activity designated to a scent. The mitral and tufted cells are responsible for relaying this information to the olfactory cortex. Mitral cells only extend dendrites to a single glomerulus, thereby maintaining the one odor to one neuron pathway. A single glomerulus can receive dendrites from several sister mitral cells, but the temporal activity and thresholds of these cells are different. These differences allow for odor-tuning of concentration and spatial location (Tan et al., 2010; Kikuta et al., 2013).

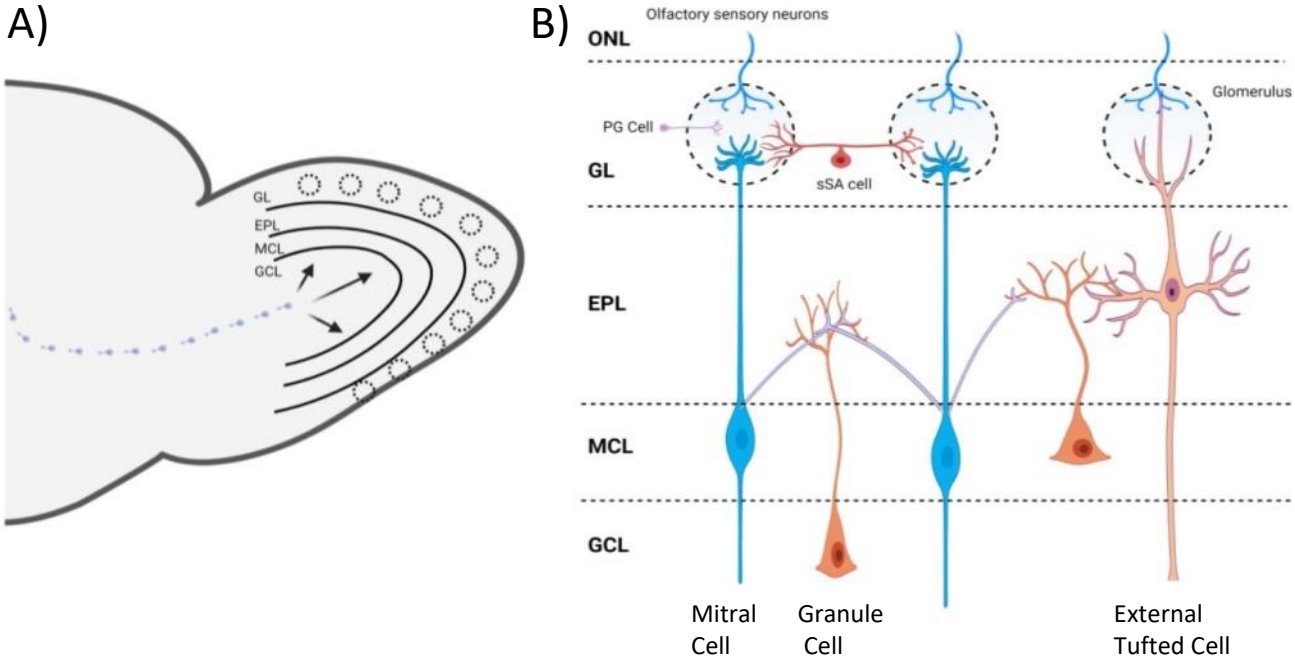

Figure 1.2) Organization of the Olfactory Bulb (OB)

The migrating neuroblasts rely on chain migration to reach the olfactory bulb, where they then switch to radial migration and penetrate into the appropriate layer of the OB. A) Sagittal view of the migratory path neuroblasts take to the OB. B) Organization of cell layers in the OB. MCL, Mitral cell layer; GL, glomerular layer; GCL, granule cell layer; EPL, external plexiform layer, ONL; olfactory nerve layer , PG; periglomerular cell, sSA; superficial short-axon cell.

1.3. Origin of the Stem Cell Pool

To study the role of *Mllt11* in the development of the SVZ neurogenic niche it is important to have an understanding of where these stem cells come from. The NSC pool undergoes fate changes according to its respective developmental stage and the environment they're kept in is just as dynamic. Following gastrulation, the three definitive layers of cells include the endoderm which forms the internal organs, the mesoderm giving rise to connective tissue and musculature, and the ectoderm which develops into the skin and nervous tissue. Formation of the neural plate is initiated when the ectoderm directly above the notochord thickens and invaginates to form the neural groove in a process called neurulation. The folds come together for the ectoderm cells to fuse and form a closed tube.

The cranial and caudal ends of the tube (neuropores) close before the fluid-filled neural tube bends to form the three primary vesicles. These enlargements on the neural tube are referred to as the prosencephalon, which develops into the cerebrum consisting of the telencephalon and diencephalon, the mesencephalon, the rhombencephalon which further develops into metencephalon and myelencephalon, and the caudal end of the neural tube which forms the spinal cord. The prosencephalon is formed in a process of bifurcation of the fluid-filled neural tube to shape into the two hemispheres. The cells lining the bifurcated bulbs constitute the earliest cortical neural progenitor cells. Homeobox genes are sequence of DNA involved in the patterning of development. Many homeobox genes have been studied for the patterning of the neural tube. One such gene is

Emx1/2 which is expressed as early as embryonic day 9 (E9) and is restricted in expression to the dorsal prosencephalon which gives rise to the pallial cortex consisting of the olfactory bulb, cortical layers, and cerebellum (Moore and Iulianella (2021); Boncinelli et al., 1995). Otx2 is another homeobox gene expressed in the rostral brain of embryos. However, Otx2 expression gradually disappears from the cortex after E10.5 whereas *Emx2* expression continues during gestation and is restricted to the germinal zone of the ventricular zone (VZ) (Boncinelli et al., 1995).

1.4. Formation of the Cortex

The most rostral enlargement of the neural tube is called the prosencephalon and it further delineates into the diencephalon and telencephalon. As the cells of the neural tube proliferate, they align themselves according to a gradient of transcriptional factors. Emx2 and Pax6 transcriptional gradients determine the mediolateral axis of the telencephalon (Muzio and Mallamaci, 2003; Bishop et al., 2000). The diencephalon consists of deep cerebral nuclei such as the thalamus, hypothalamus, amygdala, and hippocampus. The telencephalon is the most cranial formation of the nervous system and develops into the cerebral cortex and its constituent lobes. The cerebral cortex is comprised of six phenotypically molecularly distinct layers generated by the formation of the deeper layers first and the consecutive migration of neurons and glia past these layers towards the cortical plate to generate more superficial layers (Lee, Ji Yeoun, 2019). In the earliest stage of neurodevelopment, the neural stem cells (NSCs) of the neural tube divide

into the outer marginal zone consisting of Reelin+ Cajal-Retzius cells, the pre-plate consisting of early deep layer 6 Tbr1+ cells, and the ventricular zone maintaining their stem cell qualities (Martinez- Cerdeño and Noctor, 2014; Hevner et al., 2003). The marginal zone cells release chemokines for proper alignment of migrating progenitors. An integral component to the organization of cortical layers is the establishment of glial scaffolds for migrating neuroblasts. In later stages of development, ongoing neurogenesis requires the guidance of these radial glial cells (RGCs) to reach the appropriate layer (Barry et al., 2014; Anthony et al., 2004). RGCs will be discussed in depth later but they retain their stem cell qualities and are an active neurogenic population into adulthood. The cortex is formed by the proliferation and differentiation of NSC lining the neural tube. Defects in proliferation, differentiation, or migration of these progenitor cells result in neurodevelopmental disorders including autism spectrum disorder (ASD) and schizophrenia (Guarnieri, Fabrizia Claudia et al., 2008). Malfunctions in migration result in heterotopia and mispositioning of neurons (Marin, 2012). Importantly cells of each layer have a specific transcriptional identity that defines their role in the cortex.

1.5. Ventricular Zone

As the undulating neural tube bends and folds during development it traps empty spaces which are then filled with cerebrospinal fluid (CSF) giving rise to the ventricles. The cerebrospinal fluid contains secreted factors that are crucial for the proper development of the brain and communication between different cells, creating chemical

cue gradients. CSF is secreted by the lateral ventricle choroid plexus (LVCP), and cells of the LVCP directly modulate factors present in the CSF through their specific secretome. LVCP transcriptome analysis revealed the production of hormones, growth factors, carriers, and chemokines contributing to cell cycle regulation, quiescence, axonal transport, migration, differentiation, and survival of NSCs. These factors of interest include retinol-binding protein 4 (Rbp4), Adiponectin, noggin, TGF-beta2, CXCL-13, and VEGF-A (Silva-Vargas et al., 2016). Interestingly, noggin released by LVCP is the antagonist of BMP4 found in the CSF and has been shown to remove the inhibition of proliferation and promote neurogenesis in NSCs (Ihrie et al., 2011). The walls of the lateral ventricles are lined by pinwheel structures consisting of large apical surfaces of ependymal cells and the small apical processes of NSCs (Mirzadeh et al., 2008). The chemical composition of the CSF is critical to regulating NSC activity and maintaining their stem cell identity. CSF flow is controlled through the motility of ependymal cilia. These cells are connected by gap junctions that form a selectively permeable membrane. Ankyrin3 is an adaptor protein expressed specifically on the apical surface of ependymal cells and it is responsible for the attachment of membrane proteins to the cytoskeleton. Inhibition of FOXJ1, which regulates Ankyrin3, results in reduced neurogenesis indicating that the cytoskeletal proteins responsible for barrier formation by ependymal cells are crucial to the proper activity of NSCs in the VZ- SVZ (Paez-Gonzalez et al., 2011).

1.6. Stem Cell Niche of the VZ/SVZ

Postnatally, the germinal SVZ remains one of a few neurogenic niches in the central nervous system capable of maintaining and repairing the neuronal population in the OB (Altman, 1969). Neural stem cell bodies are immersed in the diverse niche of the subventricular zone and come in direct contact with astrocytes and progenitor cells. Along with paracrine signaling, NSC activity is controlled by soluble factors in the CSF and circulatory system. NSCs consist of radial glial cells and a subpopulation of astrocytes in the V-SVZ with glial characteristics (termed B1 Cells) (Figure 1.1). These cells exhibit bipolar cell morphology by extending an apical process to the lateral ventricle and a longer basal process to vasculature. Subpopulations of NSCs generated by B1 cell division and radial glia which lose contact with the apical surface are called B2 cells and only maintain their contact with vasculature. Interestingly, B1 and B2 cell bodies are connected through gap junctions that allow for calcium waves to spread (Lacar et al., 2011). The apical process possesses a primary cilium that comes in contact with the CSF and allows for soluble factors to regulate the NSCs' activity (Figure 1.1. B). Surrounding cells contribute to the composition of the ventricular zone niche by releasing extracellular proteins. The extracellular matrix (ECM) sequesters chemical factors and allows for a steady release of essential neurotrophic factors (Melrose et al., 2021). Astrocytes typically bridge the connection between neurons and vasculature allowing for control over permeability, nutrient delivery, and waste deposition (Platel and Bordey, 2016). However, NSCs contact the blood brain barrier where they can come into contact

with released factors (Lin et al., 2019). Furthermore, NSCs have been shown to have flexible attachments to vasculature, possessing the ability to adjust their endplate in response to changes in perivascular ECM (Mirzadeh et al., 2008; Goldberg and Hirschi, 2009). B1 cells undergo asymmetrical division to produce transient amplifying intermediate progenitor cells (IPCs) termed C cells. IPCs divide 3-5 times to produce type 'A' cells which will migrate through the rostral migratory stream (RMS) towards the olfactory bulb to incorporate into the existing circuitry (Obernier et al., 2018). A-type cells are neuroblasts fated to mature into post-mitotic neurons, their migration is guided by scaffolding vasculature and trophic factors released by the niche (Platel and Bordey, 2016). A variety of neural populations are generated from the neurogenic niche according to their region of origin. Aging results in stenosis of the lateral walls of the ventricles and the gradual shift of the neurogenic niche to the dorsal horns. Although B1 cell proliferation and radial cell count are drastically reduced in adulthood, the overall neurogenesis remains relatively consistent suggesting a population of quiescent/ dormant cells which may be held in reserve (Conover and Todd, 2017).

1.7. Migration along the RMS

The RMS forms in late embryonic stages (E15 in mice) and extends from the lateral ventricles to the ependymal layer of the OB where granule cells are found. The RMS is a tubular extension of the SVZ and follows an S- shaped path (Lois & Alvarez-Buylla, 1994; Lois et al., 1996; Pencea & Luskin, 2003). Within this structure are

newborn neuroblasts proliferating and migrating to the OB to replenish the interneuron population. The morphology of the RMS differs from rodents to primates due to the trajectory the tract takes but they have both been reported to serve as a highway for migrating neuroblasts. Neurogenesis persists into adulthood and the SVZ-RMS-OB pathway has been a field of interest in this regard (Bédard & Parent, 2004; Curtis et al., 2007). Aging results in fewer migrating neuroblasts and thinning of the RMS.

Migration of neuroblasts along the RMS is mainly to the rostral end of the stream, however, live imaging has occasionally shown these cells halt and reverse directions (Nam et al., 2007). This complex mode of migration is not reliant on a glial tube at early developmental stages. This contrasts with neuroblasts of the cortex which require the guidance of RGCs (Hatten 1999). Alternatively, migrating cells of the RMS form chain-like structures by connecting to each other via gap or adherens junctions (Marins et al., 2009). This arrangement of cells appears to constrain movement primarily to the rostral end of the stream. Interestingly, transplanting neuroblasts into the SVZ-RMS disperse in random directions (Zigova et al., 1998; Yamashita et al., 2006). This is further supported by studies that have knocked-out NCAM, a cell adhesion molecule, and observed wider RMS visualized with Nissl stains (Chazal et al., 2000). Due to the cell identity of the migrating cells, it is possible to stain the RMS using doublecortin (DCX) and Nestin to identify the structure and directionality of cells. Interestingly, neuroblasts can reshape the RMS meshwork to remove impeding astrocytic processes. This function is crucial to chain migration and avoid bottlenecks in the thin RMS (Eom et al., 2010; Kaneko et al.,

2010). Therefore, the ability to extend processes and interact with both their surroundings and other migrating cells is critical to healthy migration of neuroblasts in the RMS. Knowing that *Mllt11* interacts with microtubules and stabilized forms of acetylated- α-tubulin, it fuels the question whether it serves an important function in migration in this population of cells.

Neuronal precursor cells maintain an undifferentiated and immature state after their generation in the periventricular region until they arrive at their respective destination in the olfactory bulb where they differentiate and integrate into the synaptic circuitry. Boutin and colleagues (2009) demonstrated that terminal differentiation of periglomerular interneurons correlates with the expression of the transcription factor NeuroD1, and overexpression of NeuroD1 results in appearance of ectopic neurons at the periventricular region (Boutin et al., 2010).

1.8. Formation of the Olfactory Bulb (OB)

Patterning of the telencephalon is specified through the restricted expression of transcription factors. These graded cues determine the axes by which the cortex is formed. The dorsoventral axis is distinguished by the expression of Wnt and BMP (Furuta et al. 1997; Rubenstein et al. 1999; Hébert at al. 2002; Gunhaga et al., 2003). Whereas the rostral-caudal axis is determined by FGF proteins (Fukuchi-Shimogori and Grove, 2001). Finally, the mediolateral axis is formed by Emx2 and Pax6 expression (Bishop et al. 2000; Mallamaci et al. 2000). The earliest indication of an OB is found at E12.5 in mice when the most rostral region of the predetermined telencephalon

evaginates to form a bulb. However, at a cellular level, the mitral cells which receive information from olfactory sensory neurons (OSN) develop at E10.5 - 11. The olfactory system consists of two compartments: the olfactory epithelium (OE) located in the nasal cavity and the olfactory bulb (OB) in the skull. Despite them both originating from the ectoderm, the OE develops from the olfactory placode whereas the OB is derived from the germinal zone of the neural tube. These two systems develop separately and establish connections that interrelate the function of the two compartments. It was believed that OSNs from the OE synapse onto the ventricular zone of the telencephalon to initiate the formation of the OB. This was further supported by the findings from Gong and Shipley (1995) that showed the cell cycle duration of the presumptive OB was prolonged 24 hours after the arrival of OSN input. However, more recent studies showed that OE and OB develop separately even though OSNs of Pax6 KO mice were unable to extend their axons to the telencephalon (Jimenez et al. 2000). Therefore SVZ progenitors are recruited to generate neurons in the VONS from both local and distal regulators.

1.9. Histology of the Olfactory Bulb

The diverse subtypes of cells in the olfactory bulb are classified according to their morphology, transcriptional identity, and localization. As discussed earlier, this pathway begins with odorant molecules being detected by olfactory sensory neurons present in the olfactory epithelium lining the nasal cavity. These cells extend their processes through the foramina of the spongey cerebriform plate and innervate the glomerular layer of the

olfactory bulb which rests rostroventral to the telencephalon (Simpson & Sweazey, 2013). Olfactory signals are modified by PG, sSA, and tufted cells which innervate the same glomeruli. The signal is then passed to primary dendrites of mitral and external tufted cells to be conducted to the primary olfactory cortex on the inferior surface of the temporal lobe (Figure 1.2. B). Importantly, mitral cells extend their primary dendrite to only one glomerulus and therefore obey the single odorant receptor to single projection cell rule. Processes of mitral and external tufted cells pass through the external plexiform layer (EPL) where they synapse with apical dendrites of granule cells to be selectively inhibited on their way to the olfactory cortex (Nagayama et al., 2014).

Juxtaglomerular cells (JG) are categorized into three distinct morphological cell types: PG type I, PG type II, and sSA. PG cells are molecularly heterogeneous and can express glutamic acid decarboxylase (GAD), tyrosine hydroxylase (TH), Calretinin, or Calbindin (Nagayama et al., 2014). The mutually exclusive expression of these markers has been linked to the type of PG cells. TH-positive PG cells have been reported to be Type I, whereas Calbindin or Calretinin positive cells are Type II. It is not possible to discern the percentage of each cell type against all PG cells because they do not ubiquitously stain for the neuronal marker NeuN (Panzanelli et al., 2007). Expression of GAD 65 and/or 67 is indicative of GABAergic cells, and expression of TH is linked to dopamine production (Parrish-Aungst et al., 2007). PG cell bodies are often found in the glomerular layer and constitute the largest number of juxtaglomerular cells. Superficial short-axon cells extend dendrites to multiple glomeruli and are distinguishable by their

short axons which typically terminate in the interglomerular layer. Not much is known about the transcriptional identity of these cells, but one study has identified a subtype expressing both TH and Gad67 (Aungst et al. 2003).

Mitral cells present with various morphological and electrophysiological properties. However, the most defining feature of these cells is the extension of their primary dendrite to a single glomerulus. Mitral cell bodies comprise a thin layer of the olfactory bulb called the mitral cell layer (MCL). The cells localize more to the inferior surface of the olfactory bulb with denser MCL. Mitral cells variably express HCN2, voltage-gated potassium channel, and Tbr2 (Padmanabhan and Urban, 2010; Angelo and Margrie, 2011). Deficiencies in expressing Tbr2 have been shown to disrupt the inhibitory-excitatory balance of these cells in the mouse olfactory bulb (Mizuguchi et al., 2012). As projection neurons, the processes of these cells extend large distances and undergo multiple signal modifications. Therefore, proper axon formation is critical to the function of mitral cells.

1.10. Hypothesis and Objectives

Adult neurogenesis has been intensively studied in the past few decades. The recruitment of endogenous repair mechanisms to promote neurogenesis is a fundamental question in the field. The cellular and molecular mechanisms responsible for maintaining stem cell identity and preventing exhaustion of these valuable cells remain largely unknown. By studying the genetic control of neurodevelopment and neurogenesis

we can gain a better understanding of many cognitive disorders such as schizophrenia and ASD. The maintenance of axonal projections and network integration by newborn neurons is crucial for healthy development. This study aims to elucidate the role of *Mllt11* in the neurogenic stem cells of the lateral ventricle at perinatal and postnatal stages. Furthermore, this study investigates the consequence of *Mllt11* knockout in the generation of neurons in the olfactory bulb.

Previous work from our lab has shown the restricted expression of *Mllt11* in neural tissue and its interaction with stabilized microtubules, namely, acetylated- α-tubulin (Yamada et al., 2014). Given the impact of gain of function mutations of *Mllt11* on metastasis of myeloid leukemia and its association with cellular cytoskeleton (Li et al., 2006) we hypothesized that knockout of this gene could perturb migration in the RMS. Additionally, the neurogenic niche of progenitors is a delicate environment. Progenitor cells require appropriate cell contact with the lateral ventral, which supplies nutrients to help maintain neural stem cells postnatal, ready to supply newborn neurons to the olfactory bulb. Conditional *Mllt11* loss-of-function could distort processes and impede connections between these cells and their niche leading to a loss of stem cells and reduced capacity for neurogenesis.

HYPOTHESIS: Given the recently described role of *Mllt11* in newborn neuron migration in the cerebral cortex (Stanton-Turcotte et al, 2022), I hypothesize that *Mllt11* regulated neuroblast formation and/or migration from the SVZ and in the OB.

To address this, immunofluorescence imaging was performed on postnatal day 10 and 30 brains to compare *in-vivo* tissue of mice lacking *Mllt11* to wild type strains. P10 represents early perinatal neurogenesis whereas by P30 the animals are entering into adulthood. These time points allow us to compare the role of *Mllt11* as the stem cells transition into adulthood. Additionally, stem cell cultures were performed to assess proliferation and differentiation capacity of stem cells independently of their niche environment using the neurosphere assay. This thesis set out to accomplish the following objectives:

1. Identify the expression of *Mllt11* in postnatal SVZ and OB
2. Examine cell types and density in these two regions
3. Assess migration along the RMS using EdU tracking
4. Investigate the consequence of *Mllt11* knockout on stem cell proliferation and differentiation

CHAPTER 2 MATERIAL AND METHODS

2.1. Animals

Using a conditional knockout mouse model, we examined the effects of *Mllt11* during perinatal development at times coinciding with neurogenesis in the olfactory bulb at postnatal day 10 and 30 (P10 and P30). The conditional knockout mice underwent Cre-mediated excision of the *Mllt11* locus flanked by LoxP sites. *Mllt11*$^{flox/flox}$; *Emx1*$^{IRESCre/+}$ were used to excise the gene in the entire pallial cortex, and all forebrain neural stem cell derivatives, including SVZ progenitors. *Emx1* is an early homeobox gene responsible for the patterning of the embryonic telencephalon and expressed as early as E9 (Gorski et al., 2002). The *Emx1*$^{IRESCre/+}$ allele was obtained from The Jackson Laboratory (*B6.129S2—Emx1*$^{tm1(cre)Krj}$*/J*, Strain#: 005628) (Rubenstein et al., 1999), and used to excise a conditional *Mllt11*$^{flox/flox}$ allele generated in the lab, which was recently described (Stanton-Turcotte et al, 2022). This strategy allowed us to knockout *Mllt11* in the SVZ, RMS, and OB. Paired with Rosa26tdtomato reporter transgene (*Ai9 Rosa26TdTomato* (B6.Cg-*Gt(ROSA)26Sor*$^{tm9(CAG-tdTomato)Hze}$/J, Strain#: 007909, The Jackson Laboratory), this animal model allowed for ensuring activation of Cre excision had occurred and determining the area affected in the pallial cortex (Figure 2.1). The *Mllt11*$^{flox/flox}$; *Emx1*$^{IRESCre/+}$ was maintained in the C57 background to ensure genetic integrity throughout the course of the study.

For the cell culture studies, littermate controls that were either *Mllt11*$^{flox/flox}$ or *Mllt11*$^{flox/+}$ without any Cre to mediate excision. This data was included to reduce any

external factors which could have contributed to cell culture results. All breeders were between 8 weeks to 8 months of age and caged separately when expected to deliver a litter. Timed matings were set up late in the afternoon and observed early in the morning of the following day to avoid missed plugs. Plugged females were separated from mating cages and house with at most 4 other pregnant females.

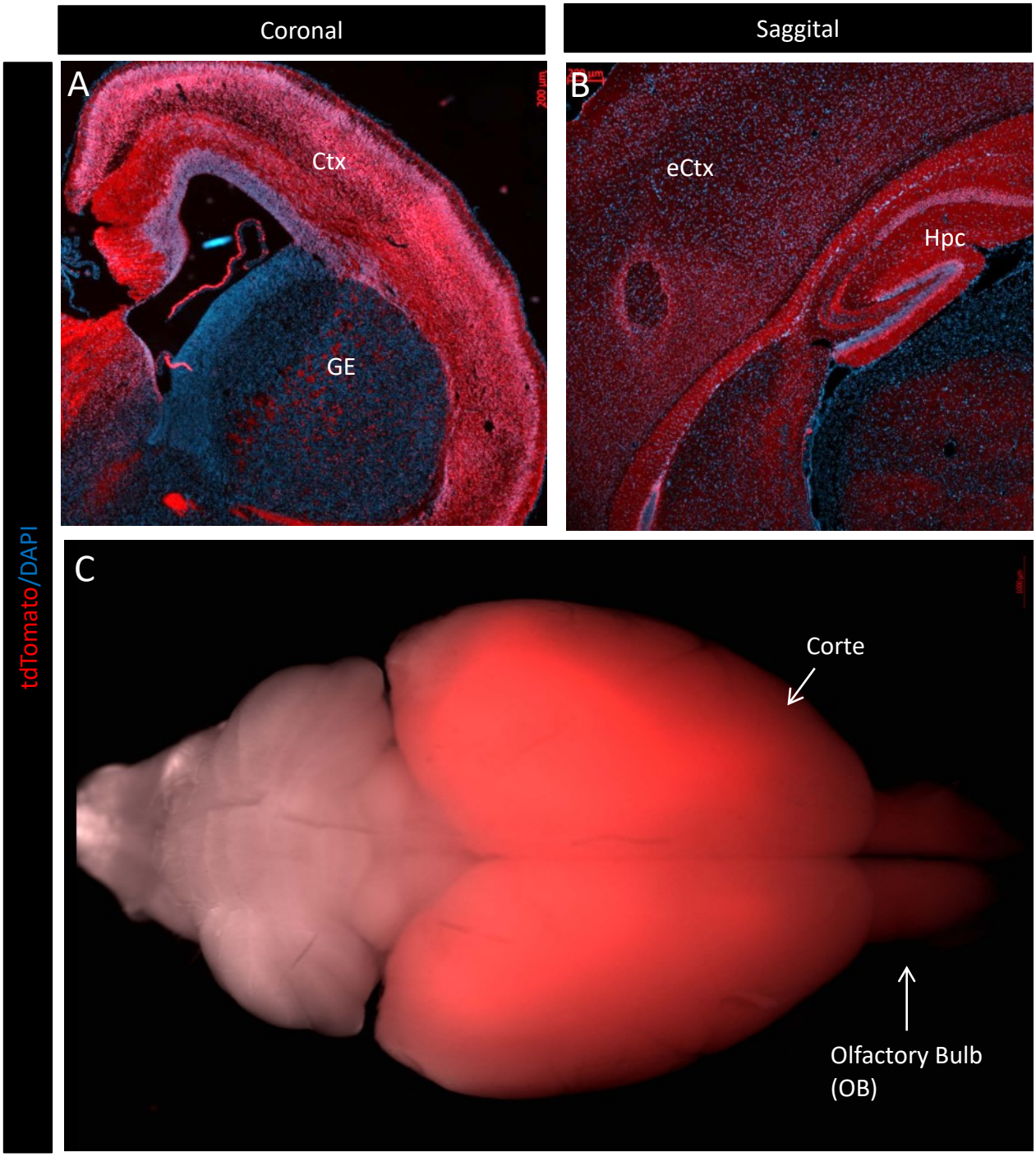

Figure 2.1) *Emx1*^{IRESCre} is Activated in the Pallial Cortex

Activation of *Emx1*^{IRESCre} visualized using a tdTomato reporter gene. On the left (A) we have a coronal view of the cortex showing activation of *Emx1* in the pallial cortex (Ctx) but not the ganglionic eminence (GE) The figure to the right (B) shows a sagittal view of the Cre activation in the hippocampus (Hpc), entorhinal cortex (eCtx), and SVZ.

2.2. EdU (5-ethynyl-2´-deoxyuridine) Labeling

EdU allows for the detection of proliferating cells and migration of their progeny due to its copper catalyzed covalent reaction between an alkyne (ethynyl) and an azide. The EdU solution was prepared at a concentration of 10 mg/ml in DMSO. Pregnant dams were dosed at 30mg/kg body weight using the 10mg/ml administered via intraperitoneal injection. Dams nearing birth were separated into single cages to account for the genotype and date of birth of each litter. The azide is coupled to Alexa-Fluor 488 dye to visualize using a Zeiss AxioObserver fluorescence microscope.

The EdU reaction to couple the azide and fluorescent marker was conducted using the Click-iT EdU imaging kit (Invitrogen). The Click-iT reaction included the Click-iT reaction buffer, CuSO4, Alexa Fluor 488, and reaction buffer additive for 30 minutes. The slides were rinsed with 3 x 10 minutes PBS before adding primary antibodies and continuing with immunohistochemistry protocol.

2.3. Cell Culture

Neurosphere Assay

P10 pups were decapitated with surgical scissors and the brain was extracted and kept in HBSS containing 1% penicillin and streptomycin at room temperature. A cut was made down the midline of the cortex to separate the two hemispheres. Two incisions were made on the medial surface of the brain in continuation with the corpus callosum to separate the cortex from the underlying hippocampus and walls of the lateral ventricles.

The dorsal horn of the lateral ventricle was dissected bilaterally and transferred to test tubes containing 1ml Neurocult's Complete Proliferation Media consisting of Neurocult basal media (45ml), Neurocult Proliferation Supplement (5ml), 1% Pen/Strep (500µl of 100X), rhEGF [20ng/ml], and FGF [10ng/ml]. Cells were mechanically triturated by pipetting P1000 X40 and P200 X20 to create a single-cell suspension. Cell density was counted by transferring 10ul of the cell suspension with equal volume trypan blue mixture to a hemocytometer. Bright cells in each quadrant were counted and averaged between the four corners. To calculate the final density of the cell suspension the average count was multiplied by the dilution of cell mix (x2 for trypan blue) and multiplied by 10^4 for the number of cells in 1ml of cell suspension.

6 well plates containing 2 ml Neurocult's Complete Proliferation Media were used to plate the neural stem cells for primary proliferation. Cells were plated at a 10 cells/µl density and incubated at 37˚ C with 5% CO2 for 7 days without changing media to avoid disturbing the cultures. The plates were not disturbed during this time to minimize clumping and contamination. Following the 7-day incubation period, plates were viewed under Nikon eclipse TS100 light microscope to quantify the number of neurospheres. Spheres must be larger than 100 µm to be considered neurospheres. Three replicate wells were counted for each animal and all replicates presented with similar counts during the experiments.

Passaging and Secondary Cultures

Media from all replicates of an animal were collected in a 15ml falcon tube. Each well was rinsed with the same media to detach any adhering cell form the bottom of the well. The tubes were spun for 5 min at 180 x g (relative centrifugal force, RCF) to collect all cells at the bottom without causing cell death. Excess media was aspirated using a P1000 and the cell pellet was re-suspended in 1ml proliferation media. The pellet was mechanically triturated using x25 P1000 and ran through a 40 μm cell strainer to eliminate any clumps. Cell density was measured using aforementioned technique and a secondary culture was plated in 12 well plates with a density of 2 cells/μl or 2000 cells/well. The cells were incubated at 37˚ C with 5% CO2 for 7 days without media change. Plates were handled with care to avoid aggregation. 3-5 replicates were plated per biological sample to ensure consistency in counting.

Differentiation Assay

Adhesive coverslips were prepared on the morning of plating cells for differentiation assay since the adhesive coating required multiple hours to sediment. Coverslips were coated sequentially with Poly-D-Lysine and Laminin for 2 hours each and rinsed with PBS to prepare for plating. A coverslip was added to each well of a 24 well plate and 500 μl of differentiation media containing Neurocult's basal media and differentiation supplement (1:9) and 1% Penicillin and Streptomycin.

2.4. Immunohistochemistry

In order to capture the ventricular zone niche, the migratory neuroblasts of the RMS, and the olfactory bulb, the tissue was sectioned along the medial surface of the sagittal plane. To allow for consistent angle and depth on each section, extracted cortices were fixed in paraformaldehyde (PFA) overnight and equilibrated sequentially in 15% and 30% sucrose. A midline incision was made to expose the medial surface and the two halves of the cortex were cryopreserved for later sectioning. The tissue was sectioned at 14 μm thickness and serially mounted on 10 slides.

Cryopreserved cortices were serially sectioned on a Leica CM1850 cryostat at 14 μm thickness along the medial surface of the sagittal plane. The sections were placed on superfrost slides (VWR, Radnor, PA) and stored at –20º C in presence of desiccant. The tissue was thawed at room temperature for 5 minutes before proceeding with IHC. Sections were permeabilized by a wash in 0.1% PBT at room temperature for 10 minutes. They were blocked using 3% normal donkey serum in 0.1% PBT for 1 hour at room temperature. The excess blocking buffer was drained from each slide and primary antibodies diluted in the blocking buffer were added accordingly. Sections were stored at 4º C overnight to allow for the binding of the primary antibody.

On the following day, slides were rinsed with 0.1% PBT to wash excess primary antibodies. Secondary antibodies corresponding to the animal of the primary antibody were used to visualize the stain. Secondary antibodies were diluted in blocking buffer at a concentration of 1 in 1500 and 400 μl was added to each slide. Slides were incubated at

room temperature for an hour, before being rinsed with 0.1% PBT 3 times and adding the nuclear stain DAPI (4'6-diamidino-2-phenylindole; Sigma, St. Louis, MS) diluted in PBS (1 in 10000). DAPI was kept on the slides for 5 minutes before rinsing with PBS and mounting the slides with coverslips and Dako Fluorescent Mounting Medium. Images were captured using a Zeiss AxioObserver fluorescence microscope at multiple axial levels and exported as Tiff files for analysis.

Table 1) Primary antibodies used:

Antibody	**Manufacturer**	**Catalogue #**	**Dilution**	**Purpose**
Tubb3	BioLegend	801201	1:1000	Intermediate filament marker of neurons
Tbr2	Abcam	Ab23345	1:250	Marker of mitral cells in the OB
Sox2	Santa Cruz	Sc17320	1:250	Marker of NSCs in the SVZ
GFAP	Abcam	Ab5804	1:500	Marker of NSCs in the SVZ
DCX	Abcam	Ab18723	1:500	Intermediate filament marker of migratory neuroblasts

Antibody	**Manufacturer**	**Catalogue #**	**Dilution**	**Purpose**
Nestin	Santa Cruz	21247	1:200	Intermediate filament marker of newborn neurons
Calretinin	Sigma-Aldrich	MAB1568	1:500	Marker of OB interneurons
Parvalbumin	Abcam	Ab11427	1:500	Marker of OB Interneurons
β-gal	Abcam	Ab134435	1:500	Reporter gene used to visualize *Mllt11* expression

Table 2) Secondary antibodies used:

Antibody	**Manufacturer**	**Catalogue #**	**Dilution**
Donkey anti-goat 650	Invitrogen	SA5-10089	1:1500
Donkey anti-rabbit 488	Invitrogen	A32790TR	1:1500
Goat anti-chicken 568	Invitrogen	A11041	1:1500

Antibody	Manufacturer	Catalogue #	Dilution
Donkey anti-mouse	Invitrogen	A31571	1:1500
Donkey anti-rat 488	Invitrogen	A48269TR	1:1500
Donkey anti-rabbit 647	Invitrogen	A31573	1:1500
Donkey anti-mouse 568	Invitrogen	A10037	1:1500
Donkey anti-rabbit 647	Invitrogen	A32795TR	1:1500

2.5. Sampling Methodology

Cell counts were restricted to regions of interest (ROI) (100μm x 100μm) randomly placed along the SVZ, RMS, and OB. Cells that overlapped with the edges of the ROI were excluded. At times the ROI was rotated to have the same orientation along the edge of the OB and SVZ. A total of 6 animals per group (WT and cKO) were analyzed. Groups were further divided by sex (3 male and 3 female) and sex differences were analyzed. ROI measurements for the same animal were averaged to give a representative value for that animal (Figure 2.2).

The cell culture analysis included both Cre controls (*Emx1*$^{IRESCre/+}$) and littermate controls (*Mllt11*$^{flox/flox}$ or *Mllt11*$^{flox/+}$) to ensure consistency in the genetic background. The analysis was made on n = 6 of each group with sex differences. Due to the sensitive nature of cell cultures only n=4 cKO and n=5 WT remained for the differentiation assay which limited analysis for sex differences.

2.6. Statistical Methods

Statistical analysis was conducted using *t* tests (two-tailed) with Welch's correction. Bar charts, line graphs, and statistical testing were created using GraphPad Prism V9.0d software, with results shown as mean ± SD. In all quantification studies, significance level was set at $p \leq 0.05$ (*$p \leq 0.05$, **$p \leq 0.01$, ***$p \leq 0.001$, ****$p \leq 0.0001$).

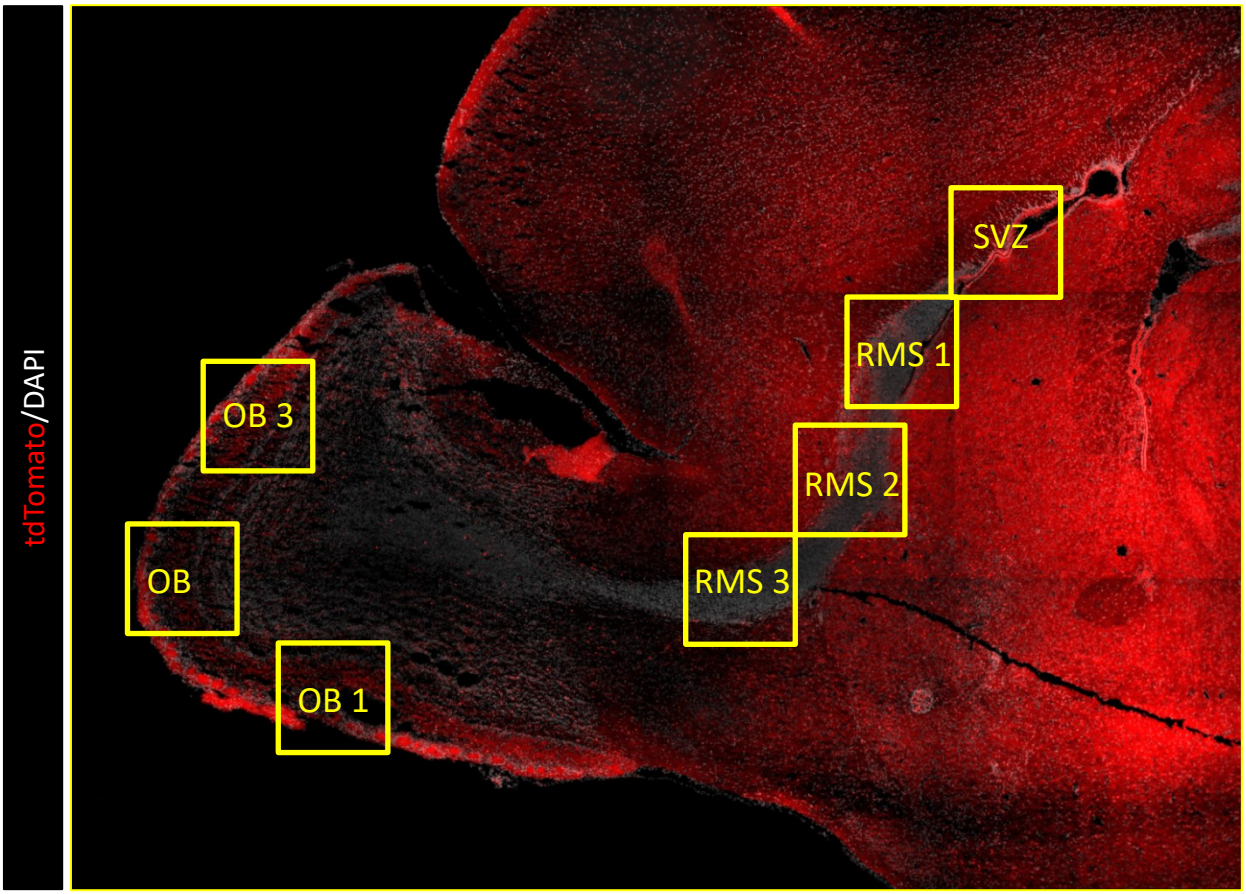

Figure 2.2) Selection of counting frames along the VONS

Regions of interest (ROIs) were drawn on each sagittal section of the brain to identify counting frames. For analysing the SVZ the region was further divided into 3 ROIs to ensure randomization of counting. Counting was done at 20x to identify individual cells. RMS, rostral migratory stream; SVZ, subventricular zone; OB, olfactory bulb. The image was acquired using tiled 10x magnification.

CHAPTER 3 RESULTS

3.1. Expression pattern of *Mllt11* and its knockout using *Emx1*^{IRESCre}

Previous work from the lab characterized *Mllt11* expression in the developing forebrain (Yamada et al., 2014; Stanton-Turcotte et al., 2022). *Mllt11* was initially detected in late fetal stages in the developing peripheral and central nervous systems and deemed a pan-neuronal marker due to its co-staining with Tubb3, a cytoskeletal marker of differentiating neurons. Yamada and colleagues (2014) reported on the co-localization of *Mllt11* expression with Tbr2 in the developing cerebrum peripheral nervous system. In the central nervous system, the gene was first detected in the telencephalon at E11.5. These cells constitute the earliest born neurons in the cortex and do not stain for Sox2, a neural progenitor marker. Recently, Stanton-Turcotte and colleagues (2022) showed that *Mllt11* is expressed in migrating neurons of the cortex at E18.5 and knockout of the gene results in delayed migration of these cells.

While these studies revealed that *Mllt11* is highly expressed in migrating and developing neurons, it is currently unknown whether *Mllt11* is expressed in neuronal progenitors within the mammalian neurogenic niche. To that end I examined the expression of *Mllt11* in the postnatal lateral ventricular/ sub-ventricular zone and olfactory bulb. I took advantage of the transgenic animal model containing a β-galactosidase (β-gal) under the *Mllt11* promoter to visualize locus activity using anti-β-gal immunohistochemistry during SVZ development. Using this approach, we found that *Mllt11* is expressed in the neurogenic niche of the lateral ventricles at P10 (Figure 3.1. A

-C), and its expression overlaps with a few Sox2-positive cells (with a ratio of 0.186 ± 0.034 $Sox2^{+}Bgal^{+}$/ $Sox2^{-}Bgal^{+}$ cells), indicating that it is present in a subset of neural precursor cells, possibly including neural stem cells (Figure 3.3. A and B). Interestingly, the cells overlapping for the two markers presented with faint Sox2 staining which could be due to a transition in identity (arrow heads, Figure 3.1. A and C). Furthermore, presence of *Mllt11* in other cells of the niche could play a crucial role in tethering progenitors to their environment and creating the appropriate connections with adjacent cells.

Mllt11 expression in the olfactory bulb was confirmed using the same β-gal strain. In this region we observed sparse staining throughout the olfactory bulb with the highest concentrated expression in the mitral cell layer (MCL) (Figure 3.2. B). The MCL lies above the external plexiform layer (EPL) and contains mitral cells that project to the olfactory cortex. These cells are crucial for relaying olfactory information and encoding odor strength and duration. The β-gal stain in the MCL overlaps with Tbr2 positive neurons (Figure 3.2. C), which is an early developmental marker of mitral cells.

Mllt11 has been shown to be a pan-neuronal marker expressed in the post-mitotic cells of the cortex (Yamada et al., 2014). Work from our lab has indicated that *Mllt11* is important to localization and appropriate migration of neurons through the cortex by regulating cytoskeletal processes (Stanton-Turcotte. et al., 2022). In the current study, we have shown that *Mllt11* is expressed in the stem cell niche of the SVZ, however, it remains unclear whether it is important to the function and identity of these cells.

Importantly, *Mllt11* was observed in a subset of $Sox2^{+}GFAP^{+}$ NSCs and primarily expressed by niche cells.

In order to evaluate the role of *Mllt11* in OB/SVZ neurogenesis, we employed the $Emx1^{IRESCre}$ driver to excise *Mllt11* in forebrain-derived neurons, include those of the OB (Briata et al., 1996). The excision was confirmed using quantitative polymerase chain reaction (q-PCR). *Mllt11* transcript levels were reduced in the olfactory bulb, but it was not significantly knocked out. This finding is attributable to the various sources of neurons in the olfactory bulb. While the $Emx1^{IRESCre}$ is an appropriate strain for targeting the palial cortex (Gorski et al., 2002) and its derivatives, the limited expression of the Cre within the olfactory bulb may lead to an incomplete knockout of *Mllt11* (Figure 3.4. B). To ensure the $Emx1^{IRESCre}$ is achieving significant knockout we sampled the telencephalon at E18.5. At this point, the outer layers of the cortex should be entirely originated from *Emx1*-expressing progenitors and therefore have undergone *Mllt11* knockout at an earlier stage (Figure 3.4. A). It is important to note that *Emx1* is expressed at a very early stage in development and may not necessarily overlap with *Mllt11* expression. However, if the excision occurs in the early progenitor cell population all descendants of those cells will also lack *Mllt11* expression. Using E18.5 cortical tissue we showed that *Mllt11* expression is significantly reduced and the $Emx1^{IRESCre}$ is a viable tool for excising *Mllt11* in the pallial cortex (Figure 3.4. A).

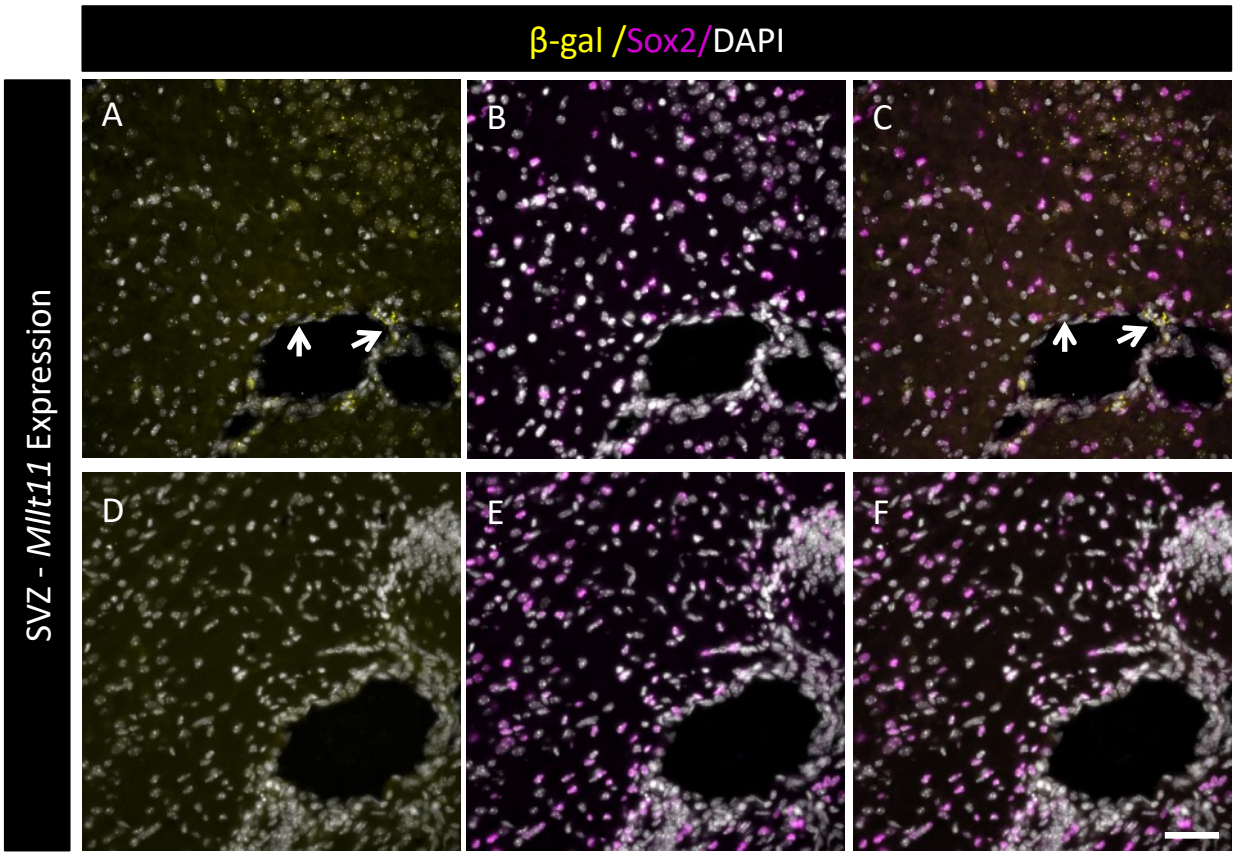

Figure 3.1) *Mllt11* expression in the ventricular neurogenic niche

Expression of *Mllt11* as visualized using a β-gal stain (Green) (A). $Sox2^{+}$ cells represent progenitor cells in the SVZ (B). Co-stain of β-gal with Sox2 (Magenta) to identify the population of progenitors in the VZ that express *Mllt11* (C). Arrows indicate cells that express *Mllt11*. Negative control of a wild type (WT) VZ showing that the β-gal staining is specific (D-F). The scale bar represents 50 μm. Images were acquired using 40x magnification.

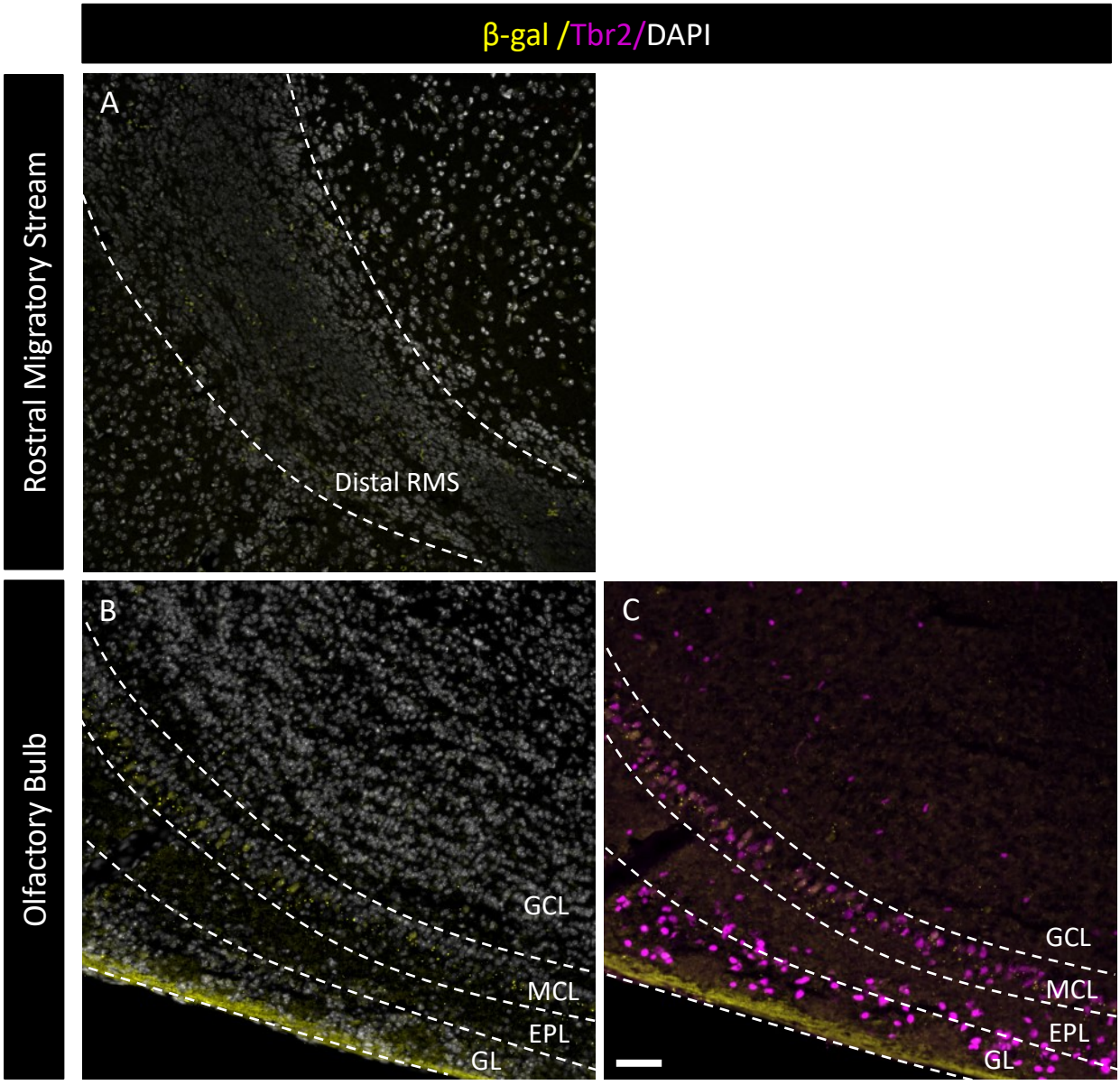

Figure 3.2) *Mllt11* expression in the Ventriculo-Olfactory Neurogenic System (VONS) Expression of *Mllt11* as visualized using a β-gal stain. A) β-gal staining (Green) in the RMS. D) β-gal staining the OB revealing the highest expression to be in the MCL. C) Co-stain of β-gal with Tbr2 (Magenta) to identify the population of mitral cells in the MCL that express *Mllt11*. The scale bar represents 50 μm. Images A and B were acquired using 20x magnification.

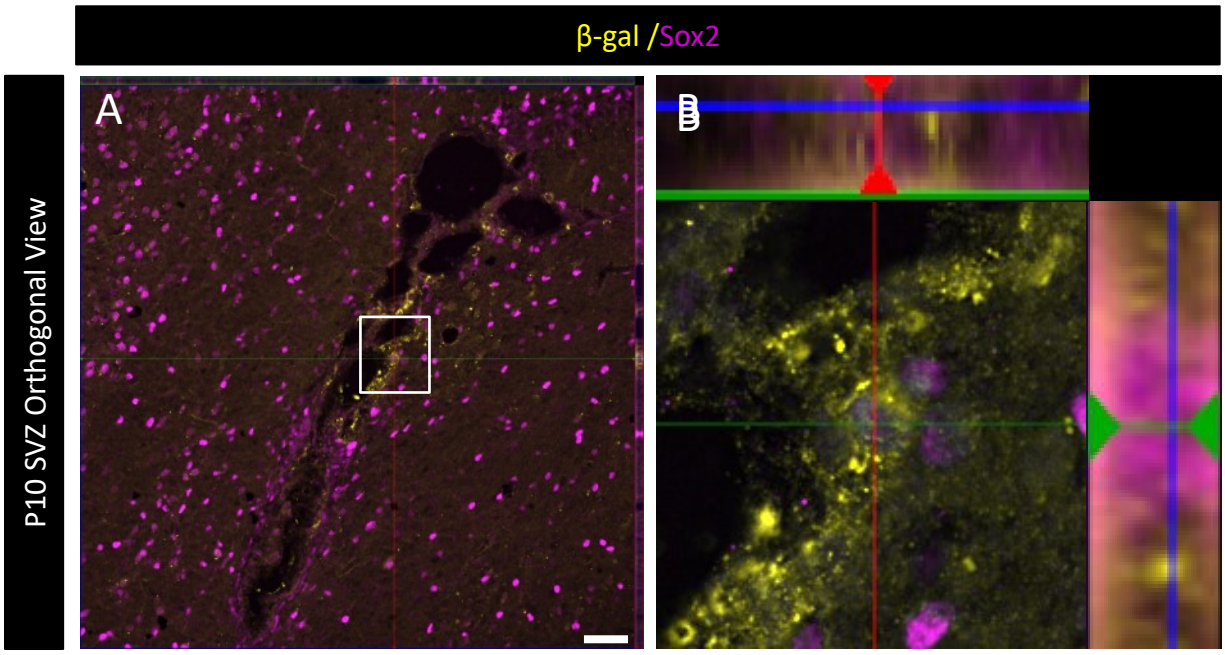

Figure 3.3) Orthogonal view of *Mllt11* expression in the VONS

A) Orthogonal view of the SVZ showing overlap of Sox2 and β-gal. B) Zoomed in view of the white box (in figure 3.2 A) and the X and Y orthogonal views showing that Bgal surrounds the Sox2 transcription factor in the nucleus. The two stains may not overlap completely due to different localization within the cell. Presence of β-gal surrounding the progenitor cells indicates the expression of *Mllt11* in those cells. It is worth noting that the β-gal stain did surround other niche cells and was not exclusive to Sox2 progenitors. In fact only a small proportion of Sox2 progenitors were positive for β-gal (*Mllt11).* The scale bar represents 50 μm.

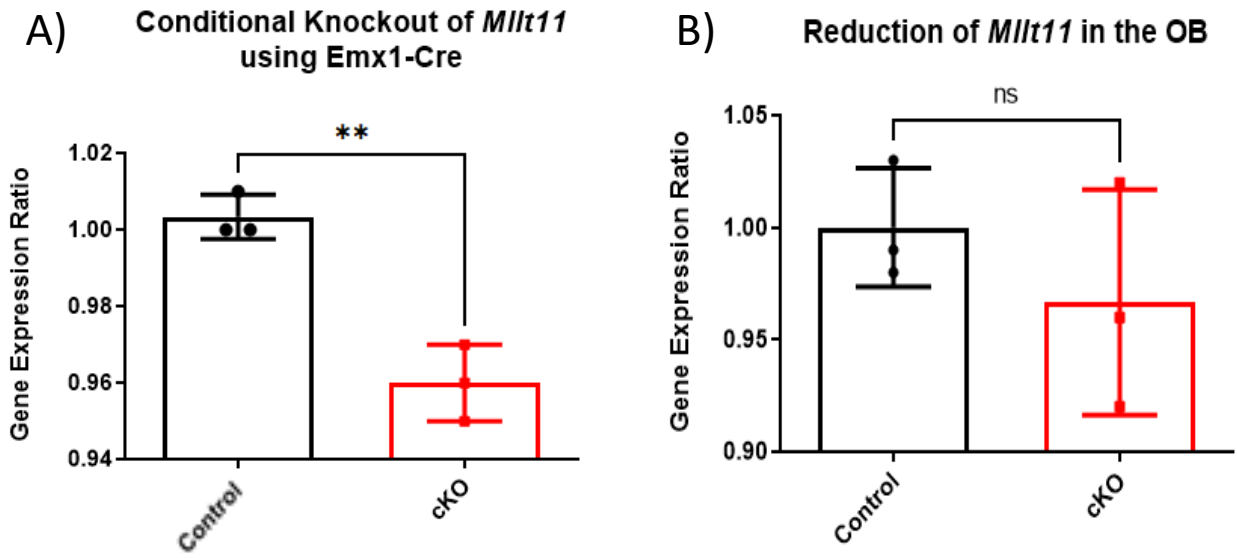

Figure 3.4) *Mllt11* expression levels using qPCR

Quantitative PCR results of the *Mllt11*$^{flox/flox}$*Emx1*^{IRESCre} cKO. A) Showing significant knockout in the pallial cortex at E18.5. B) Showing reduction of *Mllt11* expression in the P10 OB but not a significant cKO due to the variety of OB cell origins that did not express *Emx1*. The gene expression ratio was acquired by comparing expression levels of *Mllt11* to *GAPDH* housekeeping gene.

3.2. *Mllt11* knockout results in a drift of NSCs away from the SVZ region

The β-gal stain revealed the presence of *Mllt11* in the stem cell niche environment. To better understand the role of *Mllt11* on the development and localization of stem cells we examined them at P10 and P30 using Sox2 and GFAP stains. The overlap of GFAP and Sox2 at early stages of development has been shown to be an indicator of neural stem cells (Ellis et al., 2004; Imura et al., 2003). The conditional KO of *Mllt11* using $Emx1^{IRESCre}$ resulted in a wider GFAP band in the SVZ and drift away from the ventricular zone niche (Control = 0.57 ± 0.06, cKO = 1.49 ± 0.64, n=6, p value = 0.02, Welch's t-test) (Figure 3.5). The total number of $Sox2^{+}GFAP^{+}$ cells in cKO mice did not significantly change; however, the distribution of these cells was different from the controls. To quantify the changes in distribution, three regions of interest (ROI) (Control = 113.4 ± 12, cKO = 106.8 ± 7.7, n=5, p value = 0.7, Welch's t-test) were designated perpendicular to the wall of the lateral ventricle (Figure 3.6 A and B). Quantification of cell counts within these ROI revealed *Mllt11* cKO did not affect cell counts at the ventricular zone (ROI 1) but it did reduce the number of cells in the sub-ventricular zone (ROI 2) (Figure 3.6. C) (Control = 55.8 ± 6, cKO = 38.4 ± 6.4, n=5, p value = 0.047, Welch's t-test) of the lateral ventricles. The altered distribution of these $Sox2^{+}GFAP^{+}$ positive cells indicated that *Mllt11* has a role in tethering stem cells to the niche even though if it is mainly being produced by cells adjacent to the NSCs.

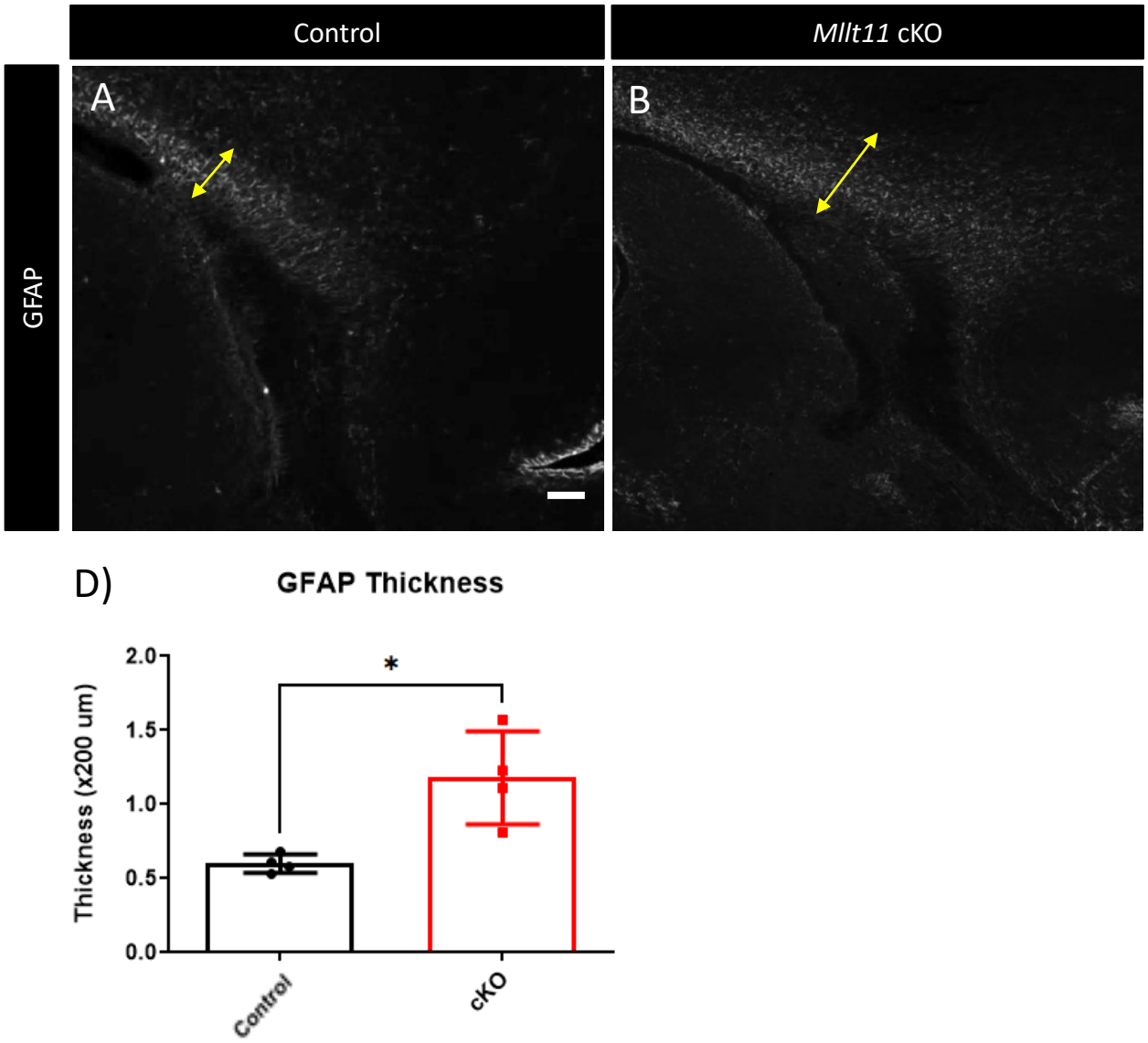

Figure 3.5) Thickness of the GFAP band at the SVZ

*Mllt11*cKO results in the expansion of the GFAP band at the SVZ. This could be a result of increased astroglia or drift of the progenitors cells of the SVZ away from the niche due to a lack of anchoring. A) A sample sagittal view of a coronal SVZ showing thicker GFAP band compared to B) sagittal view of a *Mllt11*cKO SVZ. The scale bar represents 100µm.

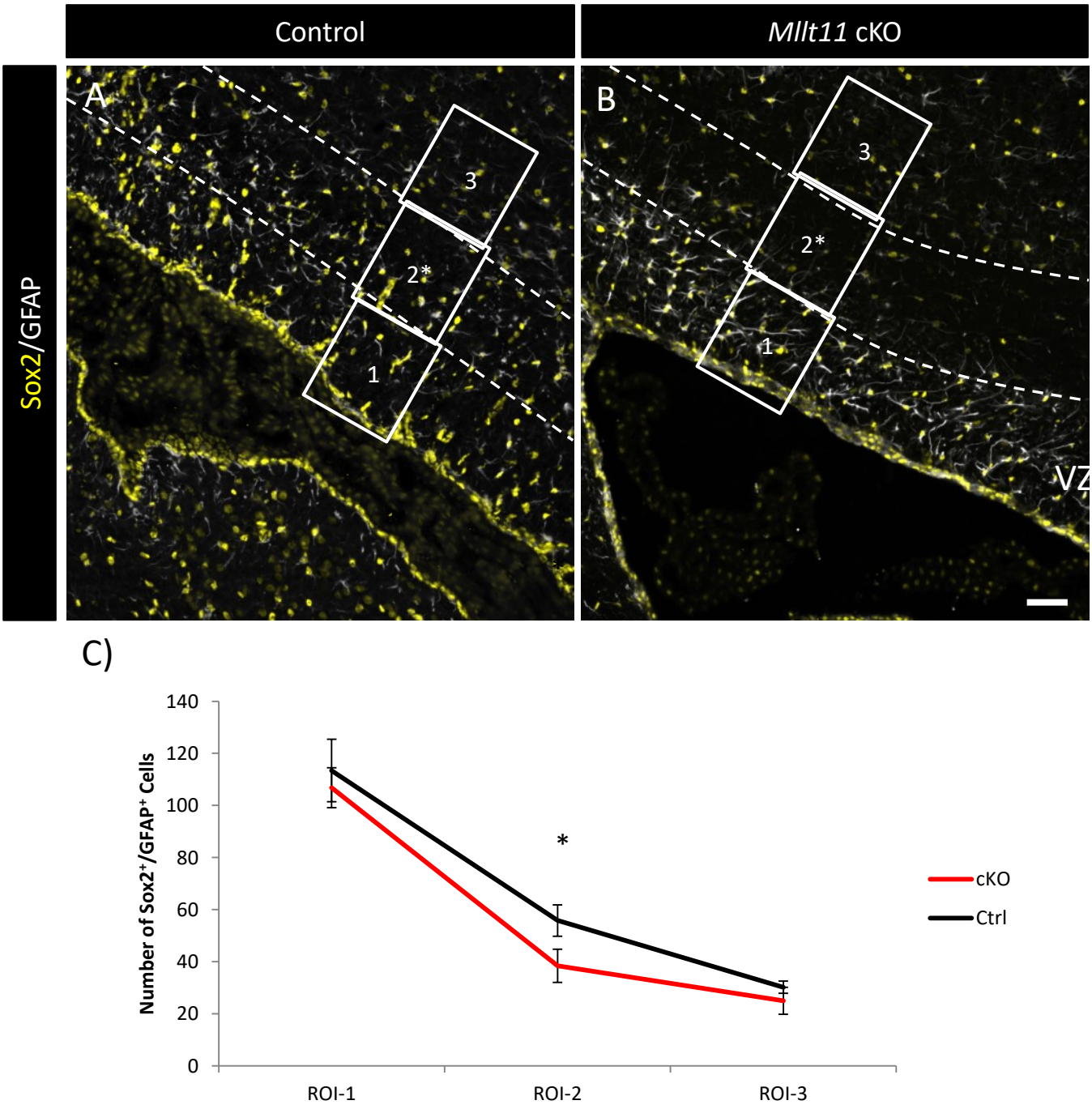

Figure 3.6) Distribution of Sox2^{+}GFAP^{+} cells in the SVZ (P30)

ROI of 100um x 100um were placed against the wall of the SVZ to bin the distribution of Sox2^{+}GFAP^{+}cells. Figure A) shows more Sox2^{+}GFAP^{+}cells in the ROI-2 of control animals compared to B) a *Mllt11* cKO. The scale bar represents 50 µm. VZ, Ventricular Zone.

3.2.1. EdU profiling of migrating neuroblasts

The niche is crucial for regulating cell cycle and cell identity in NSCs by providing factors secreted by adjacent cells, the lateral ventricle choroid plexus, and vasculature. Drifting away from the niche would likely result in a burst in proliferation and differentiation of these NSCs. In order to test this hypothesis we administered EdU (5-ethynyl-2′-deoxyuridine) to pregnant dams at E18.5 and harvested brains from P10 pups. This time frame allowed for proliferation of NSCs and recruitment of these transient amplifying progenitors and neuroblasts to the rostral migratory stream. Whiteman and colleagues (2007) have shown that neuroblasts require 10-14 days to reach the olfactory bulb and integrate within the local network. Therefore, by administering EdU at E18.5 we are providing ample amount of time for these neuroblasts to reach their destination. Interestingly, the strategy was able to pick up migrating neuroblasts and those that have reached the OB. However, there was a build-up of EdU^+ cells at the junction of the SVZ and RMS at both P10 (Figure 3.7. A and B) (Control = 61.5 ± 19, cKO = 166 ± 40, n=6, p value = 0.001, Welch's t-test) and P30 (Figure 3.8) (Control = 21 ± 3.9, cKO = 47 ± 8.9, n=6, p value = 0.0006, Welch's t-test). These results could indicate a burst in proliferation as we expected from the NSCs not being tethered to their niche, or a failure of these cells to incorporate into the RMS and migrate to their destination. Therefore, to evaluate whether the increased number of EdU^+ cells reflected increased proliferation of neural progenitors I evaluated their self-renewal *in vitro.*

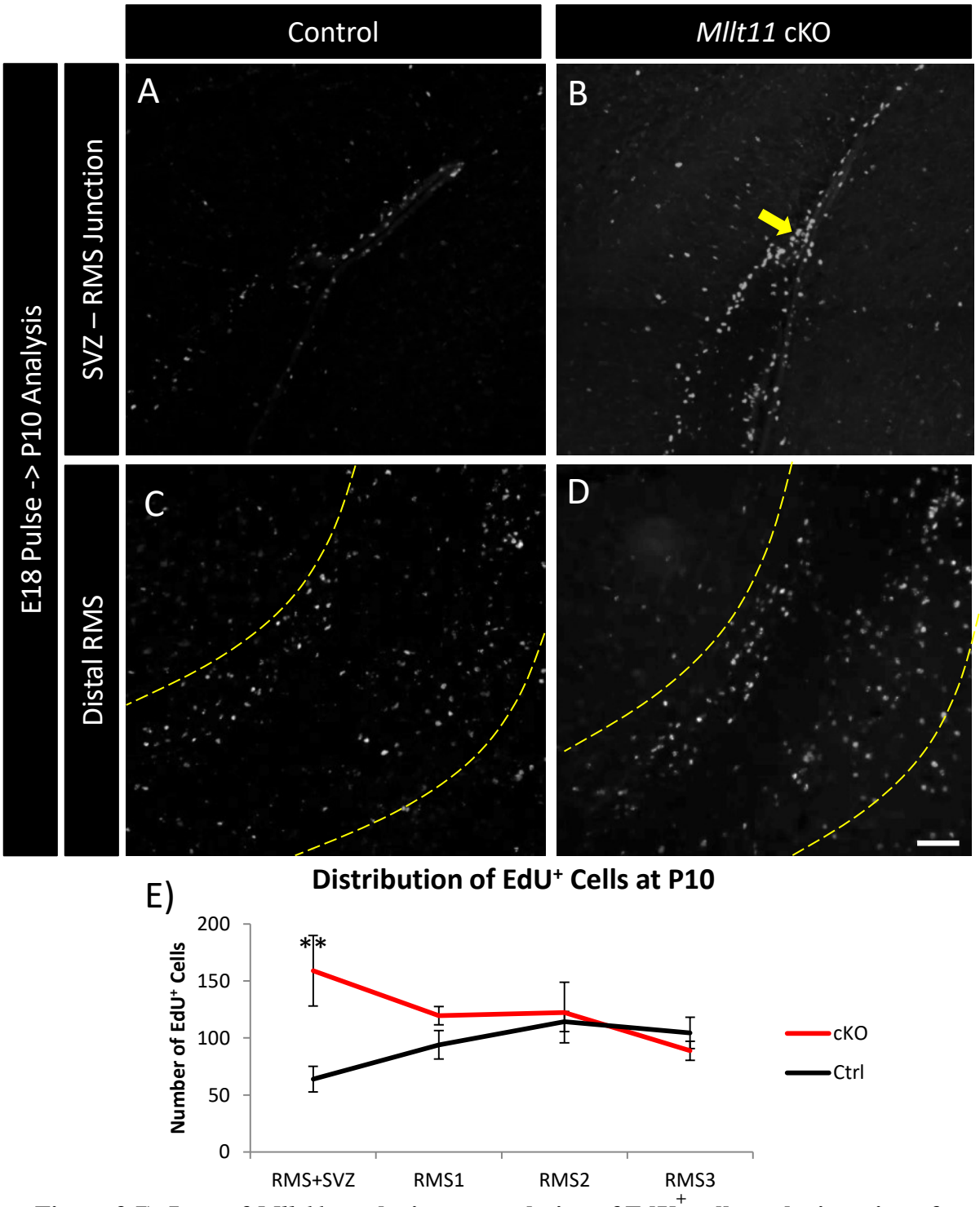

Figure 3.7) Loss of *Mllt11* results in accumulation of EdU$^+$ cells at the junction of the SVZ and RMS (P10)

Pregnant dams were injected with EdU at E18.5 and cortical tissue was collected at P10. The accumulation of EdU$^+$ cells at the SVZ – RMS junction (arrow on B) of *Mllt11* cKO animals compared to control animals (A). There is a non-significant increase in *Mllt11* cKO at the start of the RMS, however, the distal RMS did not show any differences (C and D). The scale bar represents 50 µm.

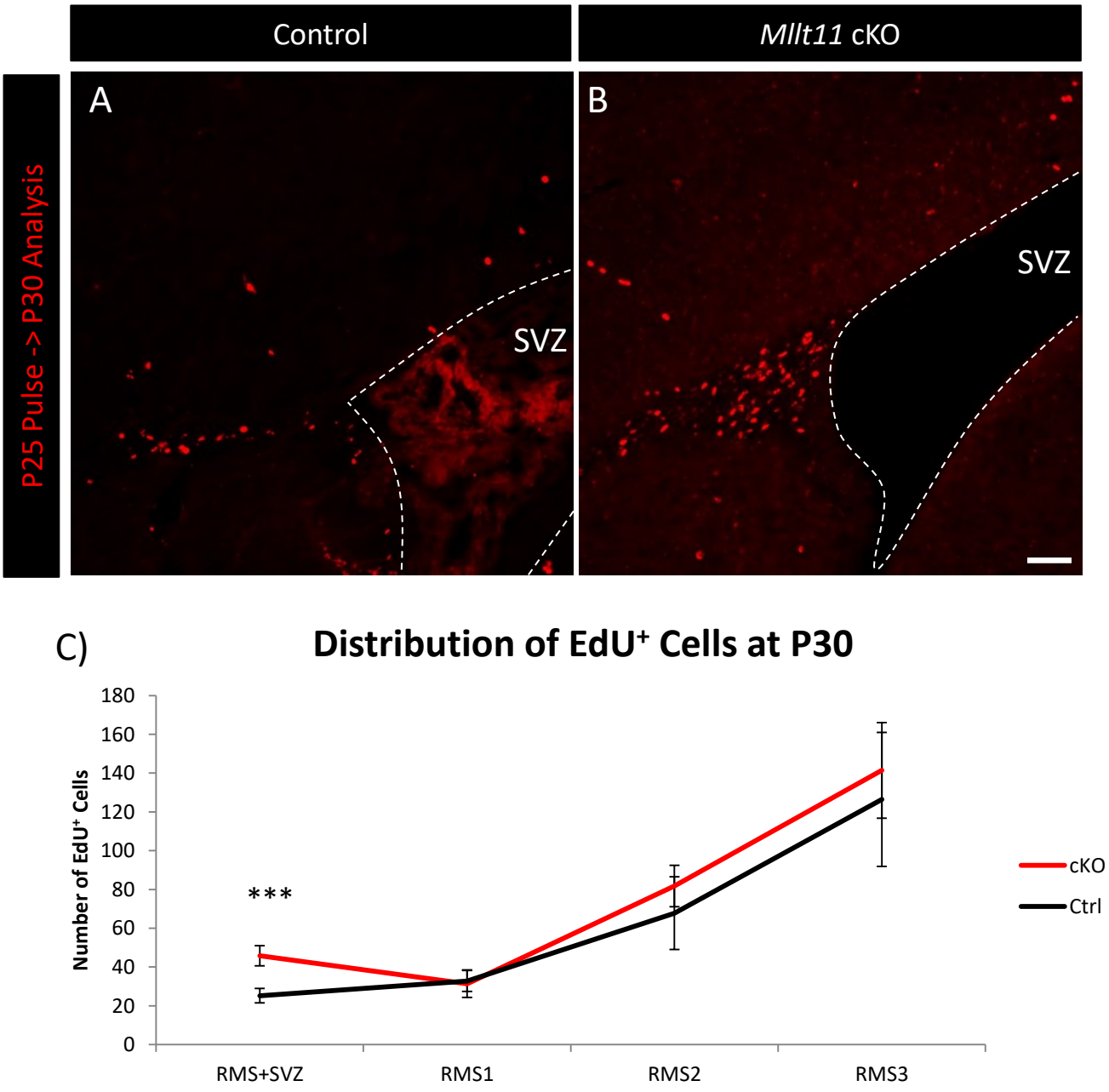

Figure 3.8) Accumulation of new born cells at the SVZ persists into adulthood (P30) Animals were injected with EdU at P25 and tissue was collected at P30 to assess distribution of EdU^+ cells along the RMS. A) Control animals presented with fewer EdU stained cells at the junction of the SVZ and RMS consistent with the P10 results. B) *Mllt11* cKO resulted in an accumulation of EdU^+ cells at the SVZ. ROI used in quantification outlined in Figure 2.2. The scale bar represents 50 μm.

3.3. *Mllt11* loss results in a deficit in NSCs' ability to self-renew

In order to assess the intrinsic effect of *Mllt11* conditional knockout (cKO) on the NSCs, I performed a neurosphere assay. This technique has been widely used to characterise the proliferative capacity of neural stem and progenitor cells. In short, the dorsal horn of the lateral ventricle was dissected bilaterally at postnatal day 10 and dissociated into a single cell suspension using mechanical trituration. The cells were then plated at a specific density in proliferation media containing fibroblast and epidermal growth factors (Figure 3.9. A). During this time the proliferative cells form neurospheres that give a quantifiable measure of the number of proliferative cells in the dorsal horn of the lateral ventricles. This initial plating of cells is called the primary proliferation assay and it measures the number of proliferative cells in the tissue. I found no significant difference between the WT, littermate controls, and *Mllt11* cKO groups in their primary proliferation (Control = 277 ± 160, cKO = 316 ± 137, n=6 control and 12 cKO, p value = 0.65, Welch's t-test) (Figure 3.9. B). This finding is in line with the *in vivo* IHC data examining the number of $Sox2^{+}GFAP^{+}$ cells. We did not expect the primary proliferation to be significantly different if the number of proliferative cells remained the same. It is important to note that the neurosphere assay does encompass transient amplifying progenitors and proliferative neuroblasts and is therefore a specific test of SVZ progenitor proliferation characteristics.

These neurospheres can be dissociated a second time and plated in proliferation media to assess the ability of stem cells to self-renew. With each consecutive passage of

neurospheres, the culture shifts towards a more homogenous and proliferative NSC population due to transient amplifying progenitors and proliferative neuroblasts being diluted out. Interestingly, the *Mllt11* cKO cultures presented with deficits in self-renewal that was quantified by the fewer (Figure 3.10) and smaller diameter spheres they formed in the secondary passage (Figure 3.11. C and D) (Control = 273 ± 48, cKO = 116 ± 41, n=6 controls and 12 cKO, p value = 0.0002, Welch's t-test). These findings are potentially due to a loss of stem cell identity in these cells and a reduced capacity to maintain their proliferative quality. The drift away from the SVZ niche would prevent the NSCs from receiving the necessary cues to maintain their stem cell identity.

No sex differences were found for the primary proliferation (Figure 3.9. C). Interestingly, the data from the secondary proliferation revealed identical results for each sex under the genetic condition. Comparison of male *Mllt11* cKO to male controls revealed a significant reduction in self-renewal as a result of the loss of *Mllt11* (Figure 3.10. B) (Control = 290 ± 54, cKO = 103 ± 32, n=3 controls and 6 cKO, p value = 0.027, Welch's t-test). Similarly, female controls produced more neurospheres in the second proliferation assay when compared to female *Mllt11* cKO (Control = 255 ± 33, cKO = 128 ± 45, n=3 controls and 6 cKO, p value = 0.009, Welch's t-test). These findings indicate that *Mllt11* function is independent of sex and corroborates the *in vivo* data at both the P10 and P30 stages.

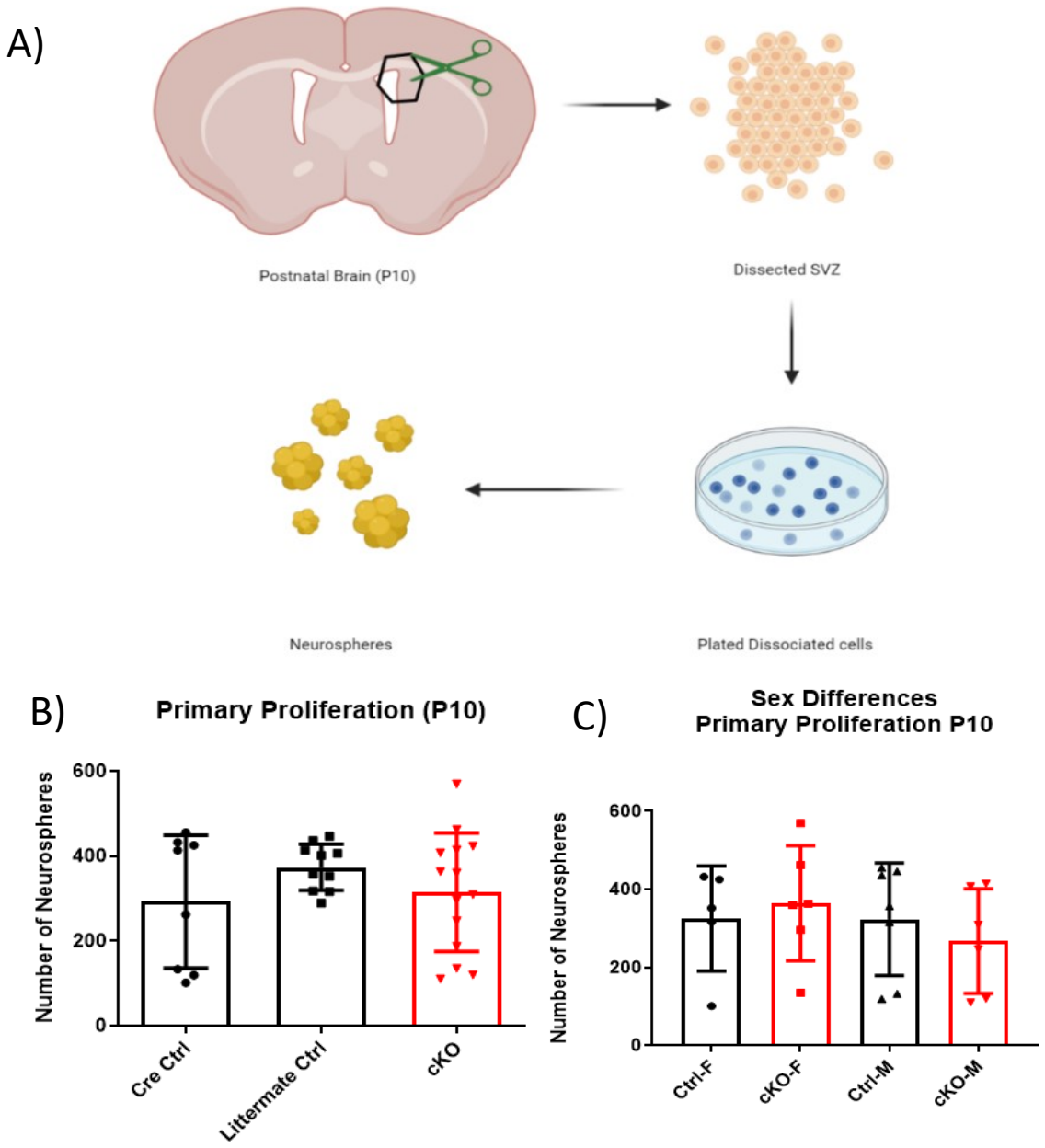

Figure 3.9) Primary Proliferation Assay at P10

The dorsal horn of the lateral ventricles are dissected bilaterally and plated as a single cell suspension to assess the number of proliferative cells (A). *Mllt11* cKO did not affect the number of proliferative cells in the SVZ (B). There were no sex differences between control and *Mllt11* cKO animals (C). The primary culture assay does not reveal the identity of the proliferative cells and therefore the secondary passage was used to quantify self-renewal and differentiation capacity.

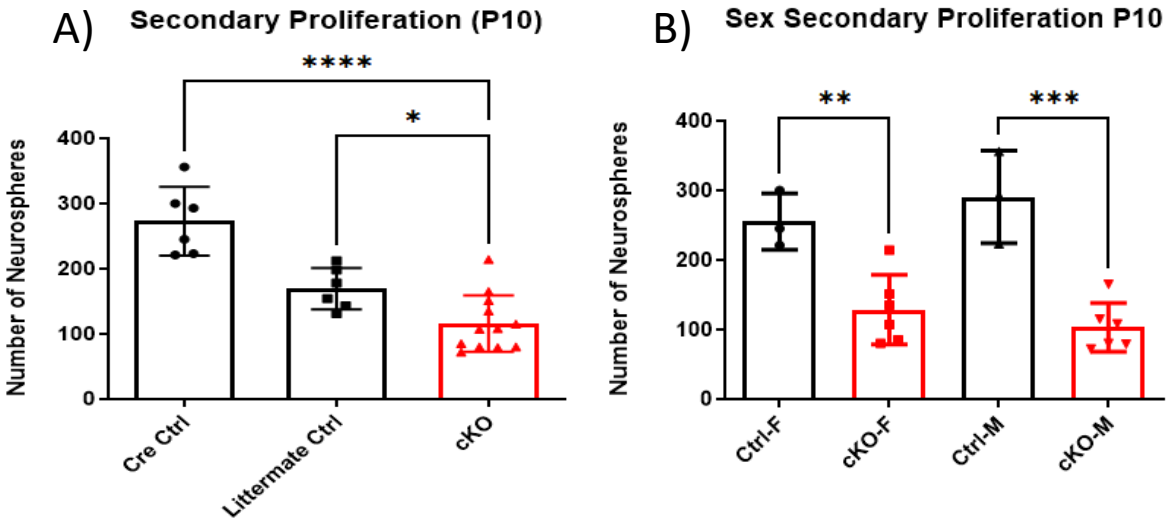

Figure 3.10) Secondary Proliferation Assay

The secondary proliferation assay is a measure of self-renewal. Consecutive passaging of the NSC culture leads to a more pure stem cell population as the transiently proliferative cells are passaged out. I found a significant deficit in the *Mllt11* cKO NSCs ability to self-renew (A). Two different controls were used to confirm this deficit, animals that only possessed the *Emx1*^{IRESCre} and littermate controls that had the *Mllt11* flox allele but lacked the necessary Cre. There were no sex differences as the mean for both males and females in each group was similar (B).

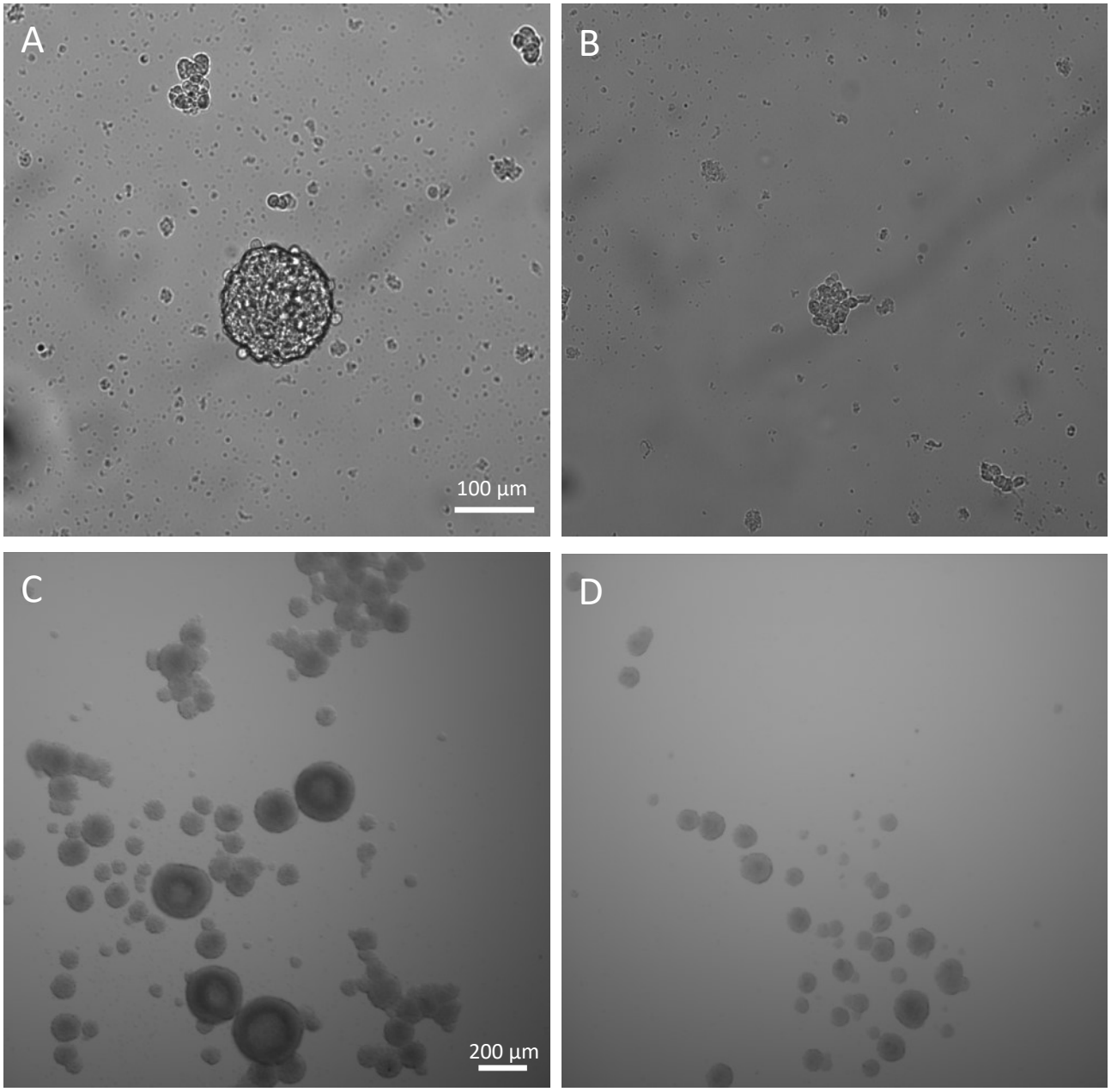

Figure 3.11) Size Exclusion of Neurospheres

Figure depicts the correct size and morphology of a neurosphere (100um diameter) on the left (A) and clusters of cells that were not included as neurospheres on the right (B). On the bottom is a representative image of a control colony (C) compared to a *Mllt11* cKO colony (D) in the secondary proliferation assay. The control neurospheres consistently formed more and larger neurospheres in the secondary proliferation assay.

3.4. *Mllt11* loss results in a deficit in NSC differentiation

Loss of *Mllt11* in the upper layer cortical neurons has been shown to alter localization and specification of upper layer neurons in the cortex (Stanton-Turcotte. et al., 2022). The phenotype of *Mllt11* cKO in the superficial cortex entailed: failure to migrate properly during inside-out formation of the neocortex, reduced axonogenesis of superficial cortical projection neurons, and reduced dendrite morphological complexity of superficial cortical projection neurons. These functions make *Mllt11* a strong candidate for affecting neural differentiation since the process requires timely signaling by the niche and development of the correct morphology by the cell. To assess the role of *Mllt11* in neural differentiation I dissociated the neurospheres from the previous experiment and plated them at 10^5 cells/ well in a 24 well plate containing adhesive coverslips.

The NSCs were cultured in base media from Neurocult in the absence of growth factors. PDL and Laminin were used to adhere the plated cells to the coverslips and initiate differentiation. Interestingly, *Mllt11* cKO resulted in a deficit in the ability of the NSCs to differentiate into neurons as quantified by Tubb3 staining (Figure 3.12) (Control = 0.23 ± 0.04, cKO = 0.08 ± 0.03, n=3 controls and 5 cKO, p value = 0.0043, Welch's t-test). Tubulin is a major cytoskeletal component and Tubb3 expression is restricted to developing and mature neuronal cells. Tubb3 antibody reacts with β tubulin- III to distinguish neurons from other cells (Ferreira and Caceres, 1992). Using this approach I was able to visualize processes of these differentiated cells which revealed the cKO cells to extend fewer processes (Figure 3.12. A and B).

Collectively, these findings suggested that *Mllt11* regulates neuronal differentiation under defined conditions in cell culture assays. Therefore, I next explored whether *Mllt11* loss lead to any abnormalities in the development and migration of newborn neurons joining the RMS to populate the olfactory bulb.

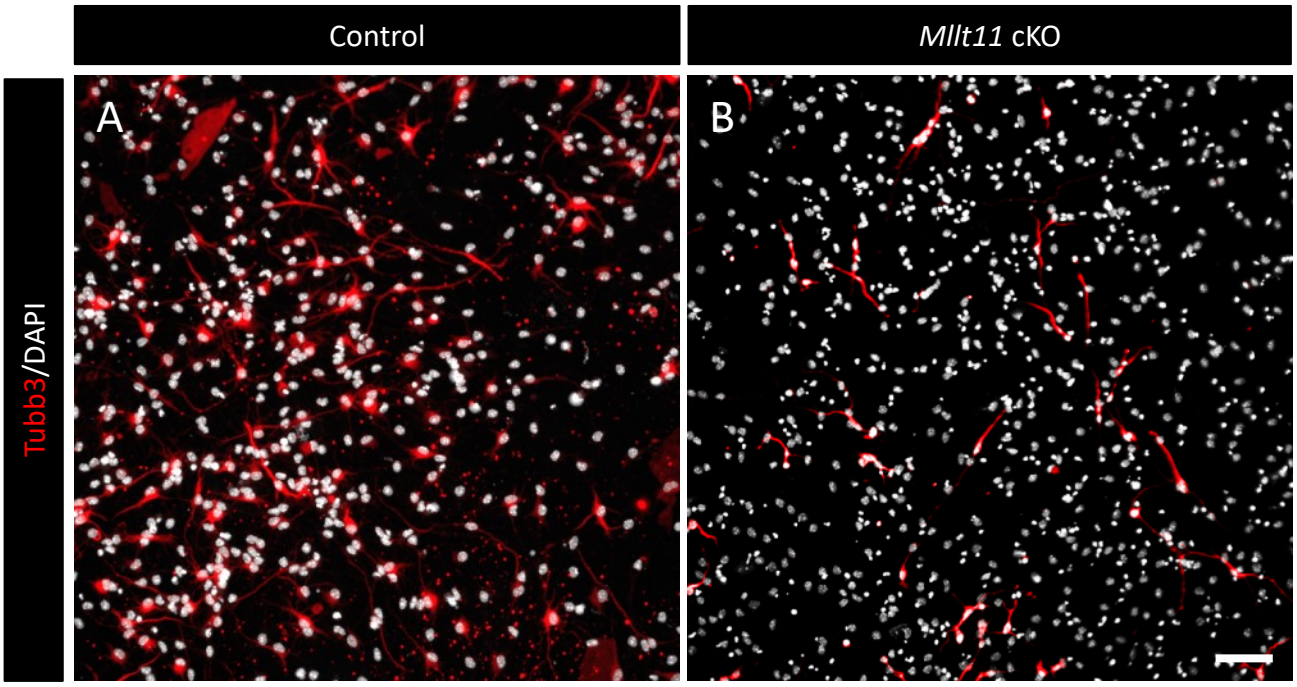

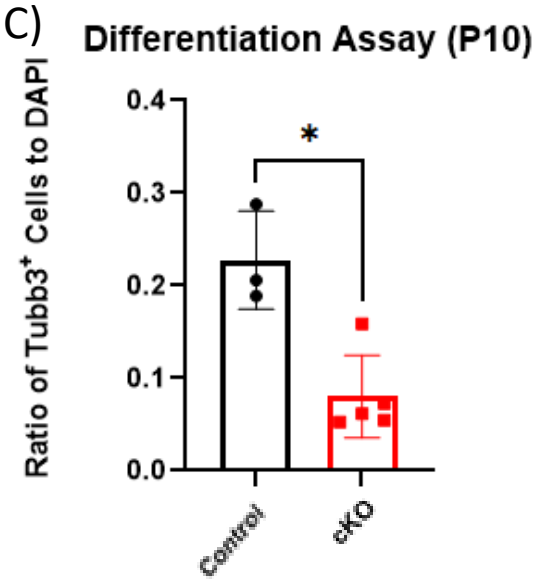

Figure 3.12) Neuronal Differentiation Assay

The neurospheres were plated on adhesive coverslips in the absence of growth factors to differentiate. *Mllt11*cKO resulted in a reduced capacity of NSCs to differentiate into neurons (C). Interestingly, the *Mllt11* cKO neurons produced fewer processes visualized using Tubb3 staining (A and B). Further supporting the role of *Mllt11* in cytoarchitecture and morphology of cells. The scale bar represents 50 μm.

3.5. *Mllt11* is not required for migration of neuroblasts along the RMS

Number of EdU labeled cells was not significantly different

To better understand the role of *Mllt11* in neuroblasts migrating through the RMS, I examined expression of *Mllt11* using β-gal as a marker. Interestingly, there were interspersed speckling of the protein along the RMS but not a significant expression (Figure 3.2. A). Whereas, in the SVZ I observed β-gal staining surrounding the $Sox2^{+}$ nucleus uniformly due to the higher expression of *Mllt11* in those cells (Figure 3.3. B). The low expression of *Mllt11* further strengthens the idea that migrating neuroblasts of the RMS are not reliant on the protein. Interestingly, the expression pattern in the OB is a combination of the speckle and nucleus surround stain which overlapped with Tbr2 staining of mitral cells (Figure 3.2. B and C). This led to studying the layers of the OB and looking at the different types of neurons that are generated from the SVZ.

To investigate the role of *Mllt11* on migration, I initially examined the RMS at P10, and then at P30 following EdU pulse-labeling of pregnant $Mllt11^{flox/flox}$; $Emx1^{IRESCre/+}$dams. Neuroblasts take approximately 5-7 days from generation in the SVZ until they reach their destination in the OB, thus labeling at E18.5 will capture the bulk of newborn neurons migrating away from the SVZ to join the RMS. At the later postnatal stage, I administered EdU at P25 and collected brains at P30. This allowed for the capturing of later stage neuroblasts populating the RMS. Quantification of EdU labeled cells along the distal RMS revealed no significant difference between WT and *Mllt11* cKO mice (Control = 114 ± 16, cKO = 122 ± 46, n=6, p value = 0.76, Welch's t-test).

The cell counts were analyzed as bins along the length of the RMS to assess distribution of cells and the analysis revealed no significant differences between WT and *Mllt11* cKO.

The distribution of EdU^+ neuroblasts along the distal RMS was further strengthened by examining Nestin (Figure 3.13) and DCX fibers (Figure 3.14) for average directionality and width. DCX is a marker of intermediate filaments expressed by migratory neuroblasts (Brown et al., 2003) and Nestin is a marker of intermediate filaments expressed by the glial bridge (Zerlin et al., 1995). This analysis revealed no significant difference between control and *Mllt11* cKO neuroblasts in their ability to extend their intermediate filaments in the absence of *Mllt11*. Average directionality is a measure of coherence of fibers to their deviation from the migratory pathway. If loss of *Mllt11* was perturbing morphology I hypothesized that these migrating cells would not be adhering to their route and either freeze, causing truncated fibers, or migrate in random directions leading to lower coherence. However, the insignificant data suggests that migration of neuroblasts along the RMS is independent of *Mllt11*. Furthermore, the width of these fibers is a direct measure of the number of cells migrating and the fact that control and *Mllt11* mutants did not differ confirms the findings from the EdU pulsing experiment showing the total number of stained cells to be the same in the distal RMS.

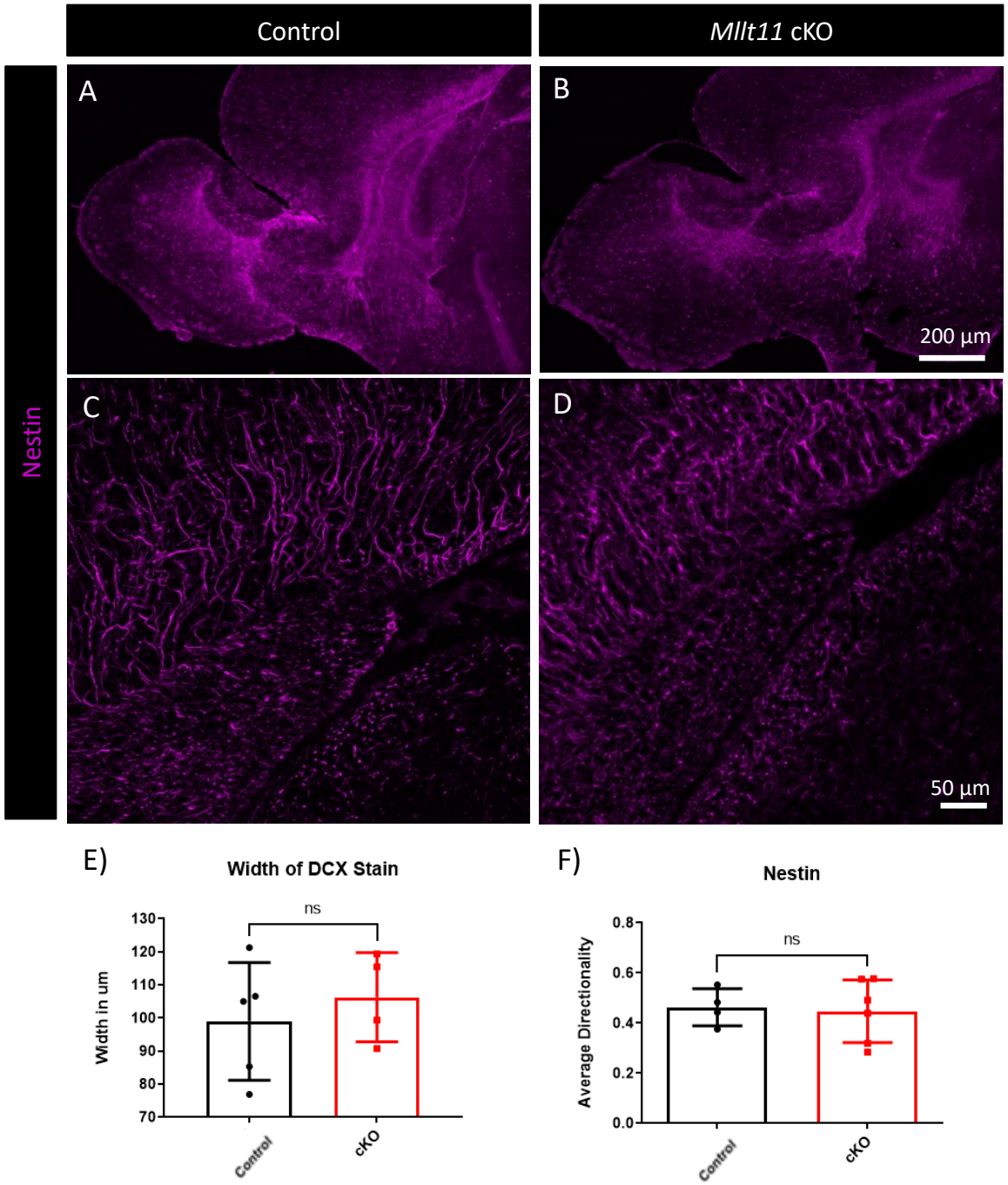

Figure 3.13) Average directionality and thickness of Nestin filaments

Nestin is an intermediate filament proteins expressed by newborn neurons. Figure A and B show no significant difference between the thickness of Nestin fibers between control and *Mllt11* cKO. Figure C and D show the directionality of Nestin filaments.

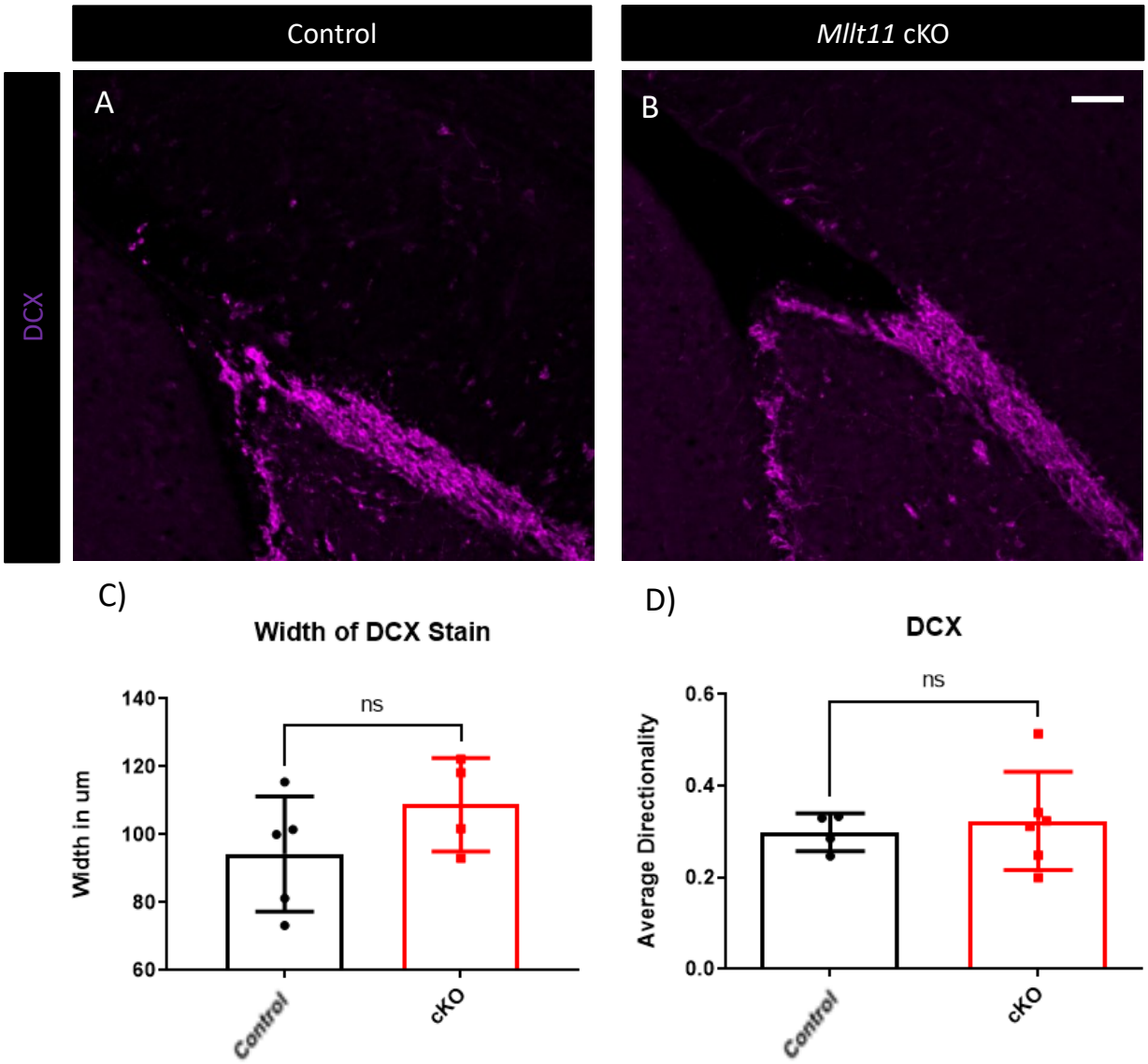

Figure 3.14) Average directionality and thickness of DCX filaments

Doublecortin (DCX) is an intermediate filament proteins expressed by migratory neuroblasts. Figure A and B show no significant difference between the thickness or directionality of DCX fibers between control and *Mllt11* cKO. The scale bar represents 50 μm.

3.6. *Mllt11* conditional knockout affects cell packing and cell fate in the Olfactory bulb

The highest expression of *Mllt11* was observed in the mitral cell layer (MCL). Mitral cells are projection neurons that transmit odor information from a single glomerulus to the olfactory cortex (Nishizumi and Miyashita, 2019). Mitral cells undergo various transcriptional changes when maturing into projection neurons. In their progenitor stage these cells are positive for GFAP and Sox2 but as they mature in the OB they express a transcriptional factor called Tbr2 (Mizuguchi et al., 2012). In order to quantify the number of maturing mitral cells in the OB I used a Tbr2 antibody at P10. The quantification of this data revealed an increase in the ratio of $Tbr2^+$ cells in the MCL of *Mllt11* cKO animals (Figure 3.16) (Control = 0.09 ± 0.03, cKO = 0.21 ± 0.06, n=6, p value = 0.006, Welch's t-test). Additionally, the MCL of cKO mice presented with a lower cell density as quantified using DAPI staining to identify cell nuclei (Figure 3.15) (Control = 87 ± 14, cKO = 65 ± 12, n=6, p value = 0.021, Welch's t-test). These findings implicate *Mllt11* in cell packing and potentially progression in transcriptional identity. In addition to mitral cells, the MCL contains the soma of granule cells scattered throughout the layer. Granule cells are reported to constitute the majority of cell somas in the MCL (Frazier and Brunjes, 1988; Imamura et al., 2006). Therefore, the increased ratio of $Tbr2^+$ cells could be due to reduced number of granule cells generated by the SVZ.

Granule cells are a diverse population of inhibitory interneurons with a variety of transcriptional identities. GCs are continuously supplied to the OB by the ventricular

zone, therefore can be classified as early-born and adult born GCs. In this study I opted to examine the calretinin (CR) and parvalbumin (PV) expressing interneurons. CR is a calcium-binding protein found in early-born and adult born granule cells. CR^+ GC have been implicated in complex odour discrimination tasks and therefore are of great interest in the function of OB network (Hardy et al., 2018). Disruptions to formation of CR neurons can have downstream effects on network integration of projection and modulatory neurons. Calretinin expressing GCs have been the primary focus of renewal studies in adulthood and have the most evidence supporting their role in the OB (Batista-Brito et al., 2008; Merkle et al., 2014; Murata et al., 2011). By examining their morphology and quantity at P10 and P30 stages I aimed to unveil the effect of *Mllt11* in perinatal and postnatal neurogenesis in the OB.

Here I report that *Mllt11* loss resulted in reduced cell density in the OB at P10 and increased ratio of $Tbr2^+$ mitral cells/DAPI. In adulthood (P30) these differences contribute to a reduced number of CR^+ cells in the MCL (Figure 3.17. C) (Control = 0.092 ± 0.025, cKO = 0.044 ± 0.009, n=6, p value = 0.006, Welch's t-test) but not the GL or GCL (Figure 3.17. D) (Control = 0.081 ± 0.028, cKO = 0.06 ± 0.01, n=6, p value = 0.27, Welch's t-test). Interestingly, the PV cell population was unaffected by our knockout strategy and remained consistent between control and cKO animals (Figure 3.18) (Control = 13.8 ± 1.99, cKO = 15.2 ± 1.3, n=6, p value = 0.24, Welch's t-test).

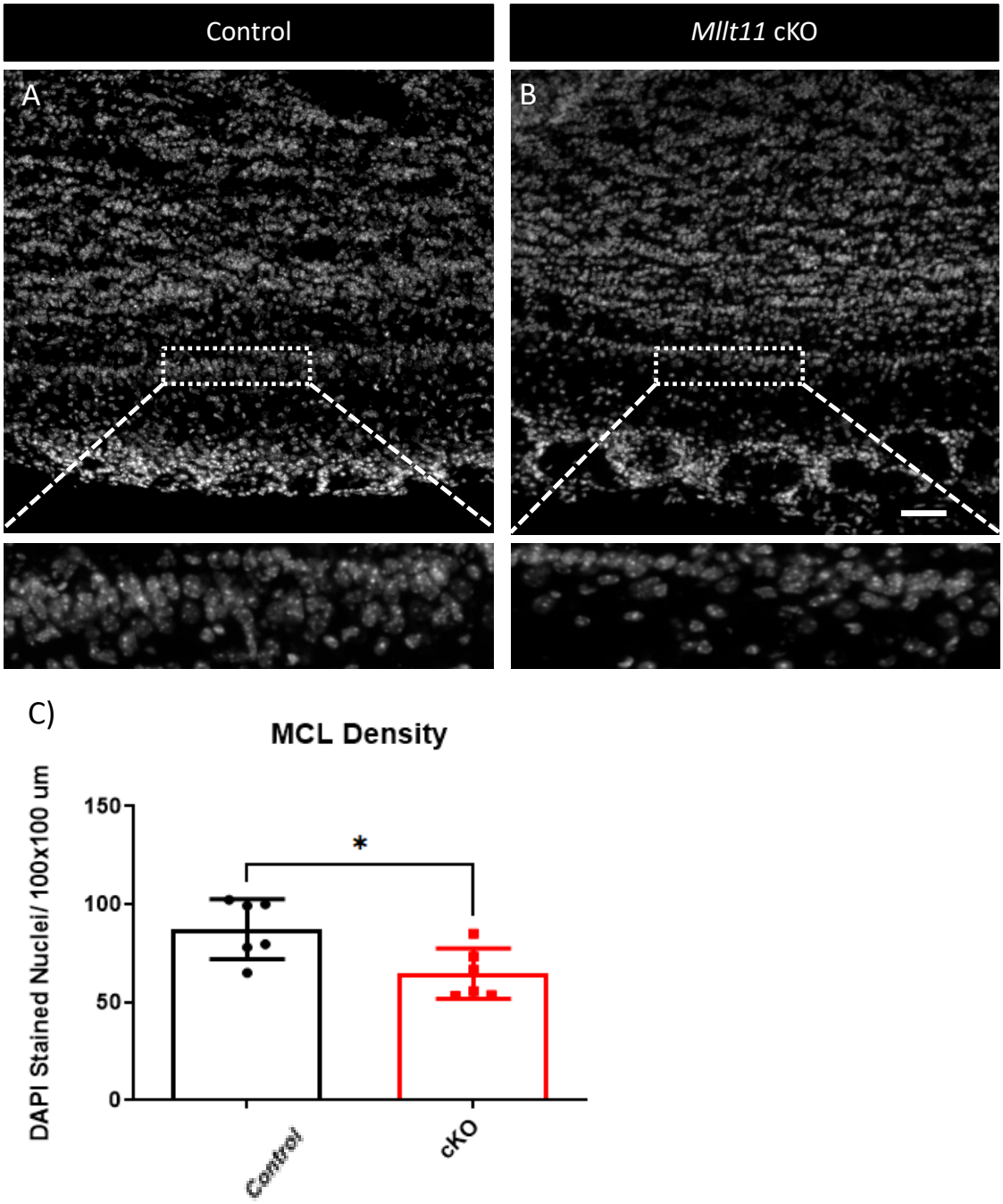

Figure 3.15) Loss of *Mllt11* results in reduced cell density in the MCL

DAPI staining of the OB revealed a deficit in cell packing in the MCL layer. A) The control OB shows neat organization of cell nuclei. B) The *Mllt11* cKO OB has disorganized localization of nuclei most likely due to loss of cell morphology. C) Quantitative analysis of cell density in the MCL. MCL, Mitral cell layer; GL, Glomerular layer; GCL, Granule cell layer; EPL, External plexiform layer. The scale bar represents 50 μm.

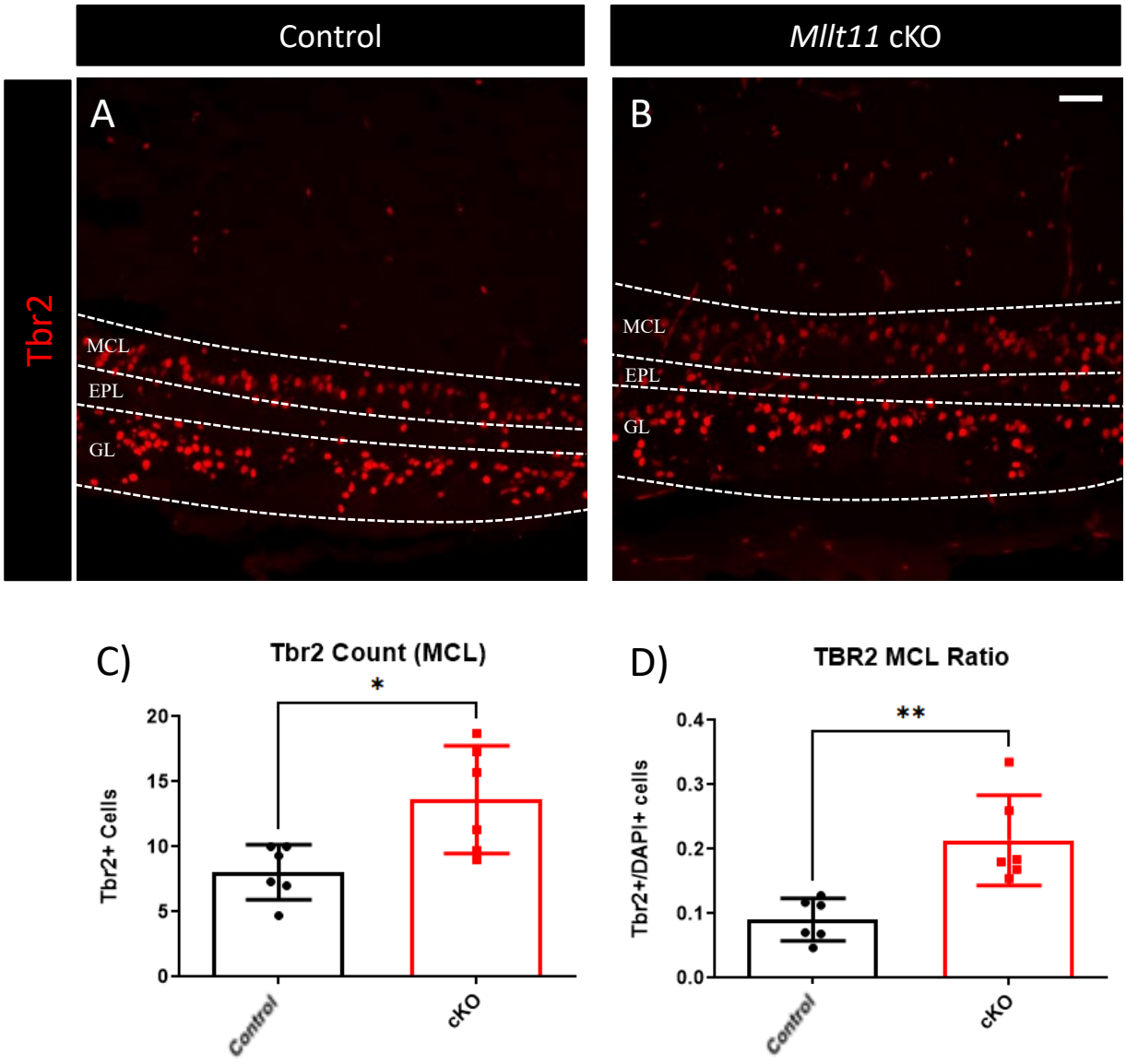

Figure 3.16) Loss of *Mllt11* results in increased Tbr2^{+} cell count and ratio in the MCL at P10

Mitral cells are projection neurons that receive information from the glomeruli and project to the olfactory cortex. Using Tbr2 staining in control (A) and *Mllt11* cKO (B) in the OB. MCL, Mitral cell layer; GL, Glomerular layer; GCL, Granule cell layer; EPL, External plexiform layer. The scale bar represents 50 µm.

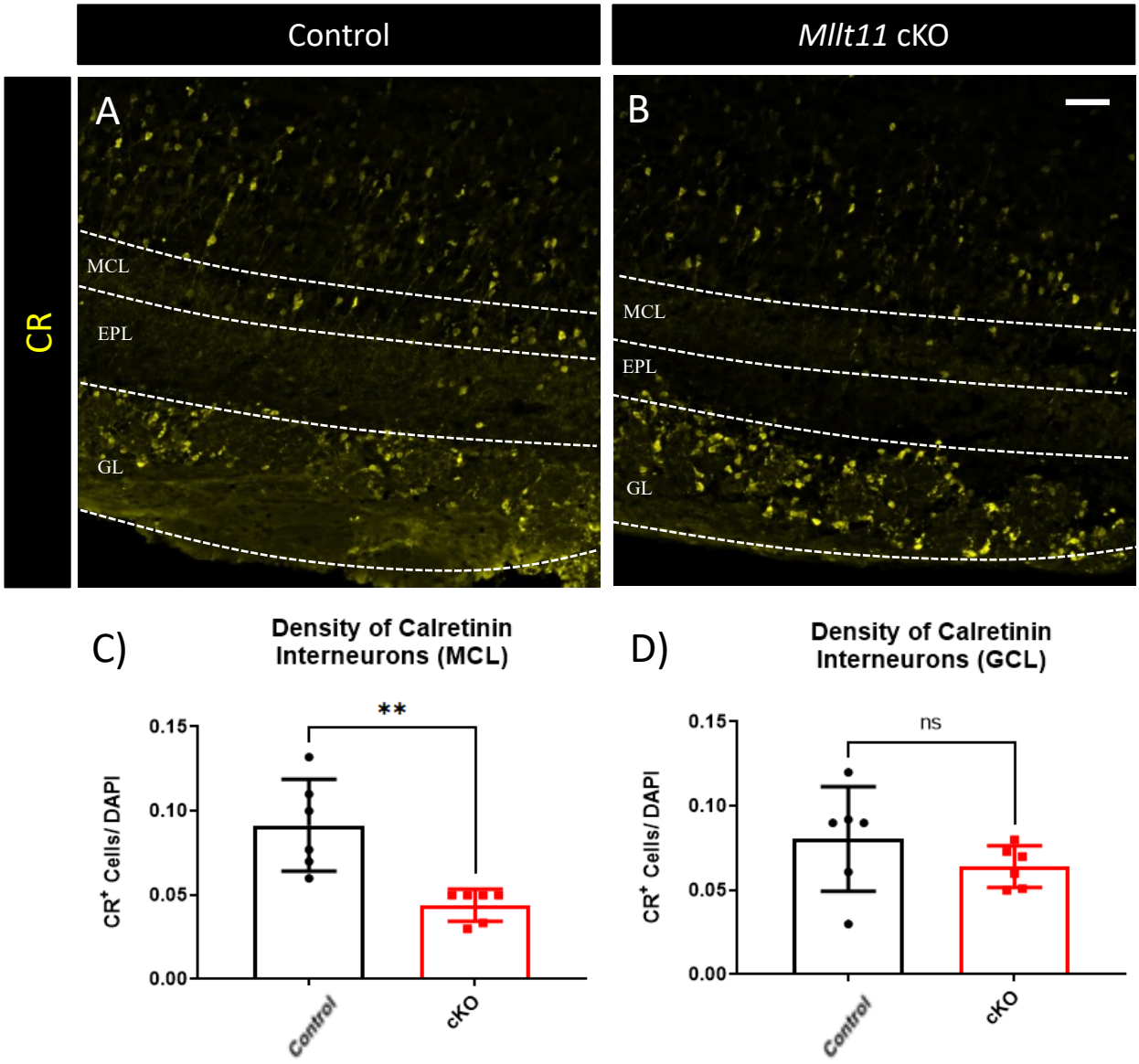

Figure 3.17) Loss of *Mllt11* results in reduced CR$^+$ cell count in the MCL at P30

Calretinin (CR) interneurons are continuously replenished by the ventriculo-olfactory neurogenic system. Therefore, loss of *Mllt11* was expected to impact their morphology and numbers. A and B show the difference in CR$^+$ cell staining between control and *Mllt11* cKO respectively. Interestingly, CR$^+$ counts were significantly different in the MCL but not the GCL or GL (C and D). MCL, Mitral cell layer; GL, Glomerular layer; GCL, Granule cell layer; EPL, External plexiform layer. The scale bar represents 50 µm.

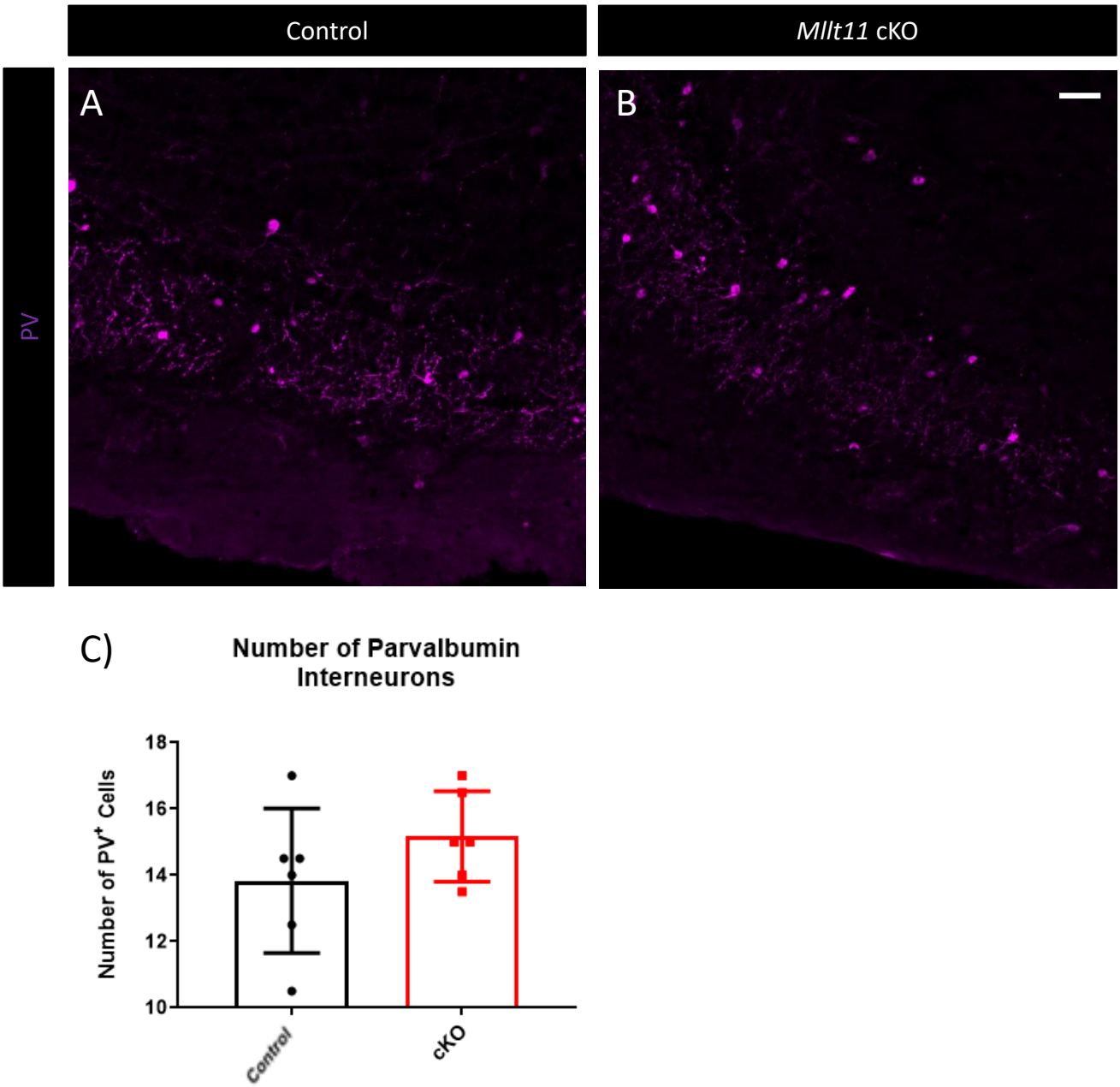

Figure 3.18) Parvalbumin expressing interneurons were not affected by *Mllt11* cKO Parvalbumin interneurons are one of the heterogeneous population of interneuron cells in the OB. PV interneurons are only generated during the perinatral stage of development. This is in contrast to the continuous generation of CR interneurons. A and B are representative images of control and *Mllt11* cKO conditions staining for PV. Although there is an insignificant increase in the number of PV^{+} cells (C). The scale bar represents 50 µm.

3.7. *Mllt11*cKO does not present with sex differences in the postnatal brain

Sexual dimorphism has been observed in the development of the olfactory system in human and rodent models (Oliveira et al., 2014; Kass et al., 2017). Although most articles allude to a non-significant difference in mass of the olfactory bulbs, they consistently report reduced number of neurons in male olfactory network. These findings have propelled the field toward discovering genetic modulators of sexual dimorphism during development. Merchenthaler and colleagues (2004) examined the distribution of estrogen receptors in the CNS and identified the estrogen receptor alpha and beta to be major contributors of hormonal activity in the CNS. Considering the role of *Mllt11* in cell cytoarchitecture and identity I was curious to see whether the deficits we observed were more severe in one sex compared to the other due to these dimorphic properties.

Sex differences were examined for all experiments except the differentiation assay. Analysis of this data revealed that *Mllt11* does not affect sexes differently and significance of data was consistent across all examinations. In most cases the group data had a more significant P value due to the larger cohort being analyzed and not due to any particular sex having more of a deficit (Table 3, in Appendix; Figure 3.9. C; Figure 3.10. B). It's worth noting that this finding pertains to postnatal brains and the *Emx1*^{IRESCre} knockout approach and does warrant exploring in the other models at earlier time points. Additionally, sex differences could be present in other parts of the nervous system but not the ventriculo-olfactory neurogenic system.

CHAPTER 4 DISCUSSION

4.1. Summary of Key Findings

The ventriculo-olfactory neurogenic system provides a compelling framework to study the role of *Mllt11* in neurogenesis, migration, and differentiation. NSCs in the SVZ neurogenic niche are under strict genetic regulation through chemical cues and physical contact with adjacent cells. The niche is responsible for maintaining the SC pool in a quiescent state and providing activation signals when neurogenesis is desired. Without these signals NSCs undergo rapid proliferation and differentiation leading to exhaustion of this vital resource (Decimo et al., 2012). In this thesis research I showed that *Mllt11* is present in the postnatal neurogenic niche of the SVZ and its cKO using an *Emx1* driven Cre results in an expansion of the progenitor domain in the SVZ. GFAP staining allowed us to observe the morphological changes in NSCs due to cKO of *Mllt11*. Furthermore, I found no significant difference between WT and cKO NSCs in their morphology using the GFAP stain suggesting that these effects could be due to supporting cells in the niche that anchor NSCs to the VZ. GFAP stains for intermediate filaments in stem cells and gives us an account of their morphology. Therefore, if loss of *Mllt11* was altering the shape of these cells we would expect to see stunted end foot processes by these cells.

To evaluate the effect of *Mllt11* cKO on the proliferative capacity of NSCs, I performed a neurosphere assay at P10. Results from this experiment elucidated that although the total number of proliferative cells was not altered, their capacity to self-renew was diminished. Additionally, the differentiation assay revealed reduced

neurogenesis and arborization by cKO cells suggesting a role for *Mllt11* in morphology and cell fate. These findings are in line with previous findings from our lab that shows a progressive loss of upper layer cortical neurons identity and reduced expression of upper layer markers such as Satb2 (Stanton-Turcotte et al., 2022). To investigate whether these differences exist *in vivo* I examined neuronal populations in the OB and found an increase in ratio of $Tbr2^+$ mitral cells due to a reduction in cell density in the MCL. The role of *Mllt11* is evident in cell packing and arrangement of the MCL. Cell density analysis allows us to control for loss of cells in the layer or the absence of newborn neurons regenerating the layer while measuring the ratio of $Tbr2^+$ cells. Using CR as a marker of granule cells I showed that interneuron populations generated from the SVZ niche are reduced in the OB.

Finally, there were no differences in DCX or Nestin staining in the RMS which was consistent with the number of EdU^+ cells across the length of the RMS not being significantly different between WT and cKO. These findings indicate that migration is not affected by *Mllt11* cKO. While I observed no significant changes in newborn neurons within the distal RMS, I did observe a significant increase in EdU+ cells adjoining the neurogenic niche in the LV. This may indicate that *Mllt11* loss did affect neuroblast emigration from the niche or that *Mllt11* loss acutely impacted neural progenitor identity in the niche, favouring a more proliferative state leading to a transient increase in neuroblast numbers. Another possibility is that these are local cells such as astroglia or mature neurons and warrants further exploration. We could distinguish between these

hypotheses using co-staining to find the identity of these cells. Using EdU along with NeuN, GFAP, and DCX (Mullen et al., 1992; Raponi et al., 2007) would uncover whether these accumulated cells are mature neurons, astrocytes, or migrating neuroblasts respectively.

4.2. *Mllt11* Expression in the SVZ Neurogenic Niche and OB

Mllt11 is present in a subset of NSCs in the niche which stain for Sox2, a transcription factor that plays a key role in maintaining stem cell identity and pluripotency. Expression of *Mllt11* in other cells in the niche presents an interesting avenue to be explored. These supporting cells could have very diverse roles such as anchoring the stem cells to the niche, providing nutrients, and balancing the composition of the ECM. The results reported in this thesis are most likely due to a combination of the role of supporting cells of the niche and the endogenous effects of *Mllt11* in NSCs. The $Sox2^{-}$ $Mllt11^{+}$ cells could also be proliferative progenitors, which are further along their differentiation path than embryonic stem cells and therefore no longer express Sox2. These proliferative NPCs are capable of contributing to the ongoing neurogenesis in the SVZ. Further work needs to be done to identify these cells and understand their exact role in the SVZ. This experiment can be approached by staining for various perinatal and postnatal markers of NPCs such as Pax6 and Tbr2 along with markers of vasculature.

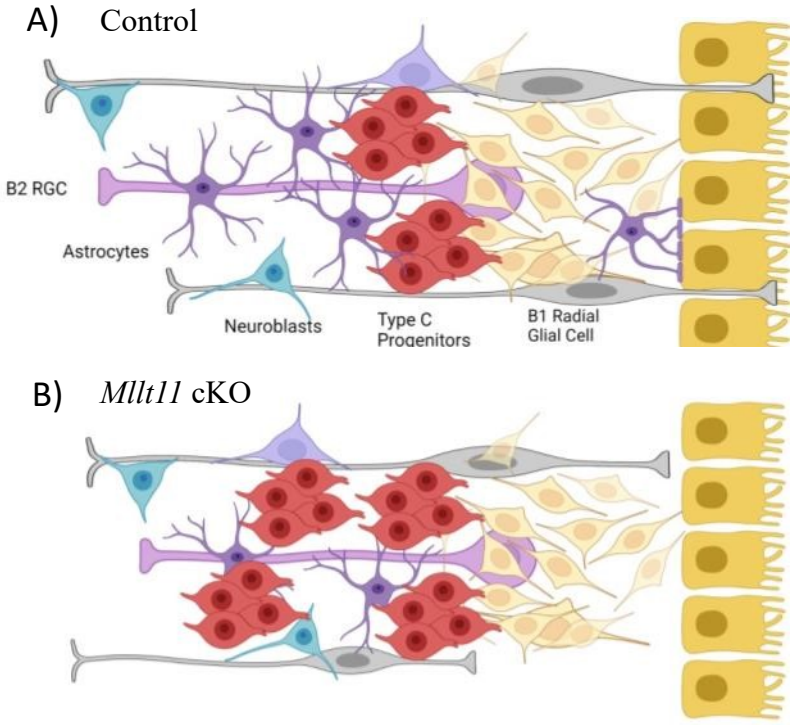

Loss of *Mllt11* resulted in:

- Expansion of the progenitor zone
- Accumulation of proliferated cells (EdU^+)
- Reduced NSC self-renewal and neurogenic potential

Loss of *Mllt11* resulted in:

- lower cell density in the MCL
- Increased $Tbr2^+$ mitral cells
- Reduced CR^+ interneurons
- No affect on PV^+ interneurons

Loss of *Mllt11* did not affect migration:

- No changes in DCX or Nestin filaments
- No changes in number of migrating neuroblasts

Figure 4.1) Summary Figure

In conclusion, loss of *Mllt11* has numerous effects on the ventroculo-olfactory neurogenic system. The neurogenic niche of the SVZ is expanded due to altered localization of NSCs and a loss of tethering. This leads to a loss of cell identity, reduced self-renewal capacity and neurogenic potential of these stem cells (A and B). There is an accumulation of EdU^+ cells adjoining the RMS, however, migration through the distal RMS is unaffected (C). At the OB, the greatest effect is in the mitral cell layer. The MCL is disorganized, and presents with greater number of $Tbr2^+$ mitral cells due to the attenuated number of CR^+ interneurons in the MCL.

4.3. Misplacement of NSCs Alters their Self-renewal Capacity

Interestingly, the total number of $Sox2^{+}GFAP^{+}$ cells was not different between WT and *Mllt11* cKO conditions . This finding is further supported by the primary neurosphere assay, which shows no differences in the number of proliferative cells in the dorsal horn of the lateral ventricles. The media conditions and the growth factors (EGF and FGF) provided in a neurosphere assay will promote proliferation if the cell is capable of it, regardless of its affinity to do so. Therefore our approach left an avenue that was left unexplored; quiescence of NSCs and whether they are held in reserve. A crucial component of the niche signalling has to do with regulating cell cycle and quiescence. Quiescence is a reversible arrest in cell cycle that allows NSCs to maintain their identity. This is different from terminally differentiated neurons or senescent cells in that they can re-enter the cell cycle (Urban et al., 2019). Quiescence can protect from accumulation of damage to DNA due to continuous proliferation and preserve the capacity of these cells to divide. If the number of $Sox2^{+}GFAP^{+}$ cells are the same between WT and *Mllt11* cKO but one group has fewer quiescent cells it could very rapidly exhaust its NSC reserve (Cheung and Rando, 2013). If *Mllt11* is indeed required to tether NSCs to the LV, then the small proportion of $Sox2^{+}Bgal^{+}$ cells could indicate that *Mllt11* expression defines a long-lived quiescent neural progenitor population in the LV. In the absence of *Mllt11* the progenitor connection to the SVZ niche is severed and as a result these cells aberrantly proliferate early in development, leading to exhaustion of the stem cell pool. It could then

be hypothesized that loss of *Mllt11* in the NSC pool can make mutant mice susceptible to insults/injuries of the OB system.

The thicker GFAP band at the SVZ along with the reduced $Sox2^{+}GFAP^{+}$ cells in the second ROI indicate that these cells drifted away from the niche. Furthermore, GFAP stains for mature astrocytes as well. Therefore, the increased GFAP band could be due to a burst in differentiation of NSCs that drifted away into astroglia. This is further supported by the reduced self-renewal capacity as demonstrated by the reduced neurosphere count in the secondary proliferation assay. Although the cells are taken out of the niche for a cell culture experiment, if the initial signalling that determined cell fate did not reach the NSC it could have lost its stem cell qualities. These results could be investigated *in vitro* using a differentiation assay. It would be interesting to examine whether loss of *Mllt11* biases NSCs to differentiate into different cell lines. The goal of this thesis was to investigate the role of *Mllt11* on neurogenesis and the results showed a clear deficit in generation and arborization of neurons. The reduced number of neurons further supports that these NSC are either differentiating into astroglia or halting in a transitory phase in differentiation which expresses GFAP.

4.4. Role of *Mllt11* in Migration along the RMS

To assess deficits in migration and track formation, proliferating cells were stained with a pulse of EdU at E18.5 and harvested brains at P10. Additionally, migration was assessed in early adulthood (P30) by pulsing with EdU at P25. This timeframe

allowed for neuroblasts to initiate their migration along the RMS. Interestingly, the total number of EdU^+ cells along the RMS was not significantly different between WT and *Mllt11* cKO. This finding was corroborated by the DCX and Nestin staining showing no difference in the absence of *Mllt11*. DCX and Nestin are cytoskeletal markers of transitory neuroblasts. I had initially hypothesized that due to the interaction between *Mllt11* and acetylated- α- tubulin (Stanton-Turcotte et al, 2022) the morphology of these migratory cells would be altered leading to deficits in making the appropriate connections in order to migrate. By analysing the DCX and Nestin stains for average directionality of fibers I was able to quantify the adherence of neuroblasts to the RMS and their ability to form the appropriate footholds to migrate. Additionally, the DCX and Nestin stains were quantified for band width to compare to EdU^+ cell counts to estimate the number of migrating cells.

These findings were unexpected because of the previous data from our lab reporting on deficits on migration in the cortex (Stanton-Turcotte et al, 2022). However, there are key differences between tangential migration along the RMS and radial migration in the cortex (Martinez-Molina et al., 2011; Nam et al., 2007). As opposed to relying on radial glial scaffolds to reach their destination, neuroblasts in the RMS form chains and are guided by chemical cues. Absence of Mllt11, a cytoskeletal interacting protein, could be greatly impacting cell-cell adhesion and foothold with the RGC, whereas it may not be as crucial for the crawling motion of tangentially migrating neuroblasts. Additionally, the cells at the tip of the chain are reported to be specialized in

detecting chemical cues and guiding the cluster. *Mllt11* may not be expressed in these cells and could explain why migration along the RMS is independent of *Mllt11* expression.

Radial migration relies on radial glial scaffold to crawl through the layers that have formed previously (Hatten 1999). On the other hand, tangential migration and specifically neuroblasts that join the RMS form chains of via gap and adherens junctions (Miragall et al., 1997; Marins et al., 2009). Neural cell adhesion molecule (PSA-NCAM) is a well-studied component of these junctions and its absence distorts and scatters cells in the chain. These findings indicate that *Mllt11* serves an important role in extension of processes and arborization more than cell adhesion. Consistently, this is also supported by the differentiation assay and the deficit in the number of processes the *Mllt11* cKO neurons created.

There was a significant increase in the number of EdU^+ cells at the junction of the SVZ and RMS indicating these cells were not recruited into the pathway. Initially I had hypothesized that these cells were a result of a burst in proliferation as the NSCs drifted away. However, the increase in EdU^+ cells at the junction of the SVZ and RMS persisted at P30. Additionally, I did not observe a burst in proliferation in the primary cell culture. Interestingly, migration was not affected by the *Mllt11* cKO, which meant that these cells are not being recruited to begin with. *Mllt11* has been shown to impact cell identity and differentiation. Conditional KO of *Mllt11* is most likely causing these cells to not develop properly and respond to migratory cues. This idea is further supported by transplantation

studies that placed SVZ NSCs in the striatum and observed dispersion of the cells, whereas transplanted mesenchymal cells in the RMS formed chain structures and showed directional migration (Zigova et al., 1998; Yamashita et al., 2006). The ability to respond to environmental cues is essential to healthy recruitment and migration. It would be very interesting to identify these EdU^+ cells and better understand why they are aggregating at the SVZ and RMS junction.

In addition to the differences between radial and tangential migration the differential role of *Mllt11* in migration in the cortex and VONS can be attributed to the stage of development. Embryonic expression of *Mllt11* is restricted to migrating neurons, whereas, I found that *Mllt11* is expressed in the neurogenic niche at P10. Postnatal role of *Mllt11* could be different than its embryonic role and instead favour the maintenance of axonal arbours rather than extension of new processes required for migration. Examining migration defects as a result of *Mllt11* cKO in other neurogenic pathways at postnatal stages can elucidate the role of this gene. Alternatively, the different roles of *Mllt11* in the cortex and VONS can be due to the Cre system used to knockout our target gene. The Cres used in this thesis and Stanton-Turcotte and colleagues (2022) have different penetrance and activity during development. As previously discussed, *Emx1* is a homeobox gene present as early as E9.5 and is responsible for patterning of the cortex. Whereas, Cux2 is expressed in SVZ progenitors and the conditional KO targets migrating upper layer cortical neurons (Stanton-Turcotte et al, 2022).

4. 5. Loss of *Mllt11* resulted in fewer differentiated neurons *in vitro* and *in vivo*

The differentiation assay demonstrated that *Mllt11* is required for the appropriate formation of neuronal processes using Tubb3 as a neuronal marker. This finding is consistent with the observations from Stanton-Turcotte and colleagues (2022) reporting on the interaction of *Mllt11* with stabilized microtubules, further supporting its role in cell cytoarchitecture and morphology. Therefore, I was interested to see whether cKO of *Mllt11* in the OB would result in the same deficits in neuronal differentiation since the interneuron population originates from the same NSC pool. The expression pattern of *Mllt11* at P10 indicated that the mitral cell layer had the highest expression of the gene. Interestingly, mitral cells are formed early in development with no evidence that they are generated later in adulthood. However, our transgenic approach allowed us to target these cells because *Emx1* expression precedes their generation. Mitral cells are formed at E11 – E13 and the cKO occurs at E9.5.

The loss of *Mllt11* resulted in a higher ratio of $Tbr2^{+}$ cells in the postnatal MCL. This finding was partly due to increased $Tbr2^{+}$ counts at P10, in combination with reduced cell density in the layer. The MCL contains the cell bodies of mitral cells and interneurons which are responsible for the lateral inhibition in the OB (Frazier and Brunjes, 1988). These interneurons are supplied to the OB throughout development and adulthood through the VONS. Furthermore, in this thesis I report that there is a reduction in the number of CR^{+} interneurons at P30 due to conditional KO of *Mllt11*. The reduced density in the MCL can be attributed to the loss of this interneuron population.

Mitral cells are generated early in development ranging from E10-13.5 (Imamura et al., 2011), whereas other projection neurons, namely tufted cells, are born at E13-16 (Hinds, 1968). The different generation times are believed to attribute to the localization of cell soma and extension of processes to glomeruli. The physical location of mitral cells determines their odorant specificity by matching them with their partner OSN axons at the glomerulus junction. If conditional KO of *Mllt11* is perturbing axonal development, it could be interfering with the pairing of mitral cells with glomeruli. Additionally, packing of these cells is important to the number of sister mitral cells that innervate the same glomerulus. Sister mitral cells have different electrophysiological properties that allow for encoding of temporal and signal intensity information (Nishizumi et al., 2019). Since mitral cells rely on lateral inhibition and sister cells to propagate olfactory signals, aberrant connections with glomeruli can have circuit-wide effects. Mitral cells have been reported to supply OSNs with trophic factors to maintain their survival.

Loss of mitral cells results in an increase in proliferation of remaining cells and TUNEL positive apoptotic cells in the olfactory epithelium (Weiler and Farbman, 1999). This feedback between the olfactory epithelium and the projection neurons is established through interneurons. The increased number of $Tbr2^{+}$ cells in the MCL due to loss of *Mllt11* could be attributed to a lack of lateral inhibition and a compensatory mechanism to innervate every glomerulus. If the density of the MCL is altered due to *Mllt11* cKO, these cells would lose their guidance and crosstalk that enabled them to innervate

different OSNs. Lack of innervation from projection neurons is associated with increased OSN and mitral cell production (Weiler and Farbman, 1999).

4. 6. Limitations

The focus of this thesis was on the role of *Mllt11* in neurogenesis at postnatal stages. To accomplish this I used an *Emx1*^{IRESCre} transgenic mouse model to cKO *Mllt11* in the pallial cortex. This strategy allowed us to target the SVZ, RMS, and OB due to the widespread expression of *Emx1* but it limited the flexibility we would have had if we had used a tamoxifen-induced model. Due to the IRES insertion of Cre it was activated as soon as *Emx1* was expressed and cleaved the flox sites flanking the *Mllt11* locus. Additionally, *Mllt11* was significantly reduced but not entirely knocked out in the mouse model. Therefore, much of the phenotype I observed was subtle and not as pronounced as the Cux2-Cre models used by Stanton-Turcotte and colleagues (2021).

Part of the difficulty of working on *Mllt11* is the lack of information and established antibodies to stain for the protein. In this study I used a β-gal stain to show the expression pattern of *Mllt11* which limited the findings to showing presence or absence of the gene in experimental tissue. In the future it would be beneficial to establish an animal model that stains for *Mllt11* to study its localization within the cell and expression level. Additionally, this approach would allow us to confirm removal of the gene in the region of interest.

A limitation of the EdU staining was the inability to distinguish between neurogenesis in the SVZ and OB due to our pulsing strategy in this study. NSCs in the RMS and OB are different from NSCs in the SVZ based on their cell cycle and differentiation potential. CR interneurons are generated from SVZ NSCs whereas dopaminergic PG originate from RMS and SVZ NSCs (Hack et al., 2005; Lledo et al., 2008). Injecting EdU locally to the SVZ would be more representative of cells generated from these NSCs. Alternatively, shorter pulse to harvest durations would show neuroblasts in transit before arriving at the OB and allow us to distinguish SVZ neurogenesis from progenitors in the OB. Additionally, we could have identified whether the EdU positive cells are migratory neuroblasts using co-stains with DCX.

4. 7. Future Direction

In this thesis I show that loss of *Mllt11* has numerous effects on the ventriculo-olfactory neurogenic system including: expansion of the SVZ neurogenic zone, accumulation of EdU^+ cells adjoining the SVZ, loss of interneuron populations in the OB, and deficits in cell packing and density in the MCL. It would be interesting to examine whether these results are corroborated by behavioural studies and if the mice present odour sensing deficits.

It is necessary to co-stain for the EdU^+ cells in order to uncover their identity. An interesting avenue that was not explored in this thesis is the effect of *Mllt11* in

astrogenesis. Astrocytes and glia play a crucial role in development of the OB and formation of the RMS. Since loss of *Mllt11* causes expansion of the neurogenic band and drift away from the SVZ niche the progenitors could aberrantly differentiate to astrocytes in the absence of the correct factors. Paired with Brainbow mice we could examine the boundaries of adjacent astrocytes to examine morphology and overlap. Brainbow uses three mutually exclusive membrane targeted fluorescent proteins to demark adjacent cells (Livet et al., 2007).

Loss of *Mllt11* resulted in a reduction of CR^+ cells in the MCL and cell density in the layer. However, it did not affect the PV^+ interneuron population or the other layers. This could be due to the temporal generation of these two interneuron populations. CR interneurons are continuously replenished and predominantly produced postnatally whereas PV interneurons are generated during perinatal stages (Batista-Brito et al., 2008). To further investigate these findings it would be interesting to use other conditional KO approaches to remove *Mllt11* in the CNS. Additionally, the *Emx1*^{IRESCre} seemed to target the mitral cells and result in an increase in their ratio. However, due to the nature of staining of these cells with Tbr2 I was unable to visualize their dendrites and axon. Tubb3 and Nestin were ineffective to identify these processes. Knowing that *Mllt11* interacts with stabilized microtubules it would be interesting to see if these projection neurons make the appropriate connections with their glomeruli and olfactory cortex.

Appendix I

Table 3) Experimental mean and P values calculated for each sexes and group data

Experiment	Male WT Mean	Male cKO Mean	Sig. Male WT vs. cKO	Female WT Mean	Female cKO Mean	Sig. Female WT vs. cKO	Group WT Mean	Group cKO Mean	Sig. Group WT vs. cKO
P10 Edu SVZ	57	149	0.09 (*)	66	183	0.012 (*)	61.5	166	0.008 (**)
P30 Edu SVZ	19.3	41.7	0.009 (**)	23	52.3	0.04 (*)	21.2	47	0.006 (**)
P10 DCX Coherence	125	117	0.59 (NS)	127	134	0.68 (NS)	126	125	0.95 (NS)
P30 DCX Coherence	0.5	0.49	0.85 (NS)	0.37	0.43	0.53(NS)	0.44	0.46	0.71 (NS)
P30 Nestin Coherence	0.32	0.28	0.51 (NS)	0.25	0.34	0.42 (NS)	0.28	0.31	0.62 (NS)
P10 GFAP Thickness	0.57	1.77	0.15 (NS)	0.56	1.2	0.09 (*)	0.57	1.49	0.03 (*)
Primary Proliferation Assay	236	268	0.8 (NS)	319	364	0.74 (NS)	278	316	0.65 (NS)
Secondary Proliferation Assay	291	103	0.27 (*)	255	129	0.009 (**)	273	116	0.0002 (***)
P10 Tbr2/DAPI MCL	0.078	0.168	0.037 (*)	0.103	0.260	0.05 (*)	0.09	0.21	0.006 (**)
P30 CR/DAPI MCL	0.114	0.038	0.004 (**)	0.069	0.04	0.033 (*)	0.09	0.044	0.006 (**)
P30 PV	12.3	15.5	0.07 (NS)	15.3	14.8	0.74 (NS)	13.8	15.17	0.307 (NS)

REFERENCES

Altman J (1969) Autoradiographic and histological studies of postnatal neurogenesis. IV. Cell proliferation and migration in the anterior forebrain, with special reference to persisting neurogenesis in the olfactory bulb. J Comp Neurol 137:433–458.

Angelo K., Margrie T. W. (2011). Population diversity and function of hyperpolarization-activated current in olfactory bulb mitral cells. *Sci. Rep.* 1 50 10.1038/srep00050

Anthony TE, Klein C, Fishell G, Heintz N. (2004). Radial glia serve as neuronal progenitors in all regions of the central nervous system. Neuron. 41:881–90.

Aungst JL, Heyward PM, Puche AC, Karnup SV, Hayar A, Szabo G, Shipley MT. (2003). Centre-surround inhibition among olfactory bulb glomeruli. Nature. 426(6967):623-9. doi: 10.1038/nature02185. PMID: 14668854.

Balu, D. T. , & Lucki, I. (2009). Adult hippocampal neurogenesis: Regulation, functional implications, and contribution to disease pathology. Neuroscience and Biobehavioral Reviews, **33**(3), 232–252. 10.1016/j.neubiorev.2008.08.007

Barry DS, Pakan JM, McDermott KW. (2014). Radial glial cells: key organisers in CNS development. Int J Biochem Cell Biol. 46:76–9.

Batista-Brito R., Close J., Machold R., Fishell G. (2008). The distinct temporal origins of olfactory bulb interneuron subtypes. *The Journal of Neuroscience.* **28**(15):3966–3975. doi: 10.1523/jneurosci.5625-07.2008.

Bédard A, Parent A. (2004). Evidence of newly generated neurons in the human olfactory bulb. Brain Res Dev Brain Res. 151:159–168.

Bishop K.M., Goudreau G., O'Leary D.D. (2000). Regulation of area identity in the mammalian neocortex by Emx2 and Pax6. Science. 288:344–49.

Boncinelli E, Gulisano M, Spada F, Broccoli V. (1995). Emx and Otx gene expression in the developing mouse brain. Ciba Found Symp. 193:100-16; discussion 117-26. doi: 10.1002/9780470514795.ch6. PMID: 8727489.

Bond, A. M. , Ming, G. , & Song, H. (2015). Adult mammalian neural stem cells and neurogenesis: Five decades later. Cell Stem Cell, **17**(4), 385–395. 10.1016/j.stem.2015.09.003

Boutin, Camille & Hardt, Olaf & de Chevigny, Antoine & Coré, Nathalie & Goebbels, Sandra & Seidenfaden, Ralph & Bosio, Andreas & Cremer, Harold. (2010). NeuroD1 induces terminal neuronal differentiation in olfactory neurogenesis. Proceedings of the National Academy of Sciences of the United States of America. 107. 1201-6. 10.1073/pnas.0909015107.

Biorender was used to create figures in this thesis (2022).

Briata P, Di Blas E, Gulisano M, Mallamaci A, Iannone R, Boncinelli E, Corte G. (1996). EMX1 homeoprotein is expressed in cell nuclei of the developing cerebral cortex and in the axons of the olfactory sensory neurons. Mech Dev. 57(2):169-80. doi: 10.1016/0925-4773(96)00544-8. PMID: 8843394.

Brown, J. P., Couillard-Després, S., Cooper-Kuhn, C. M., Winkler, J., Aigner, L., & Kuhn, H. G. (2003). Transient expression of doublecortin during adult neurogenesis. *Journal of Comparative Neurology*, *467*(1), 1-10.

.Brzustowicz LM, Hayter JE, Hodgkinson KA, Chow EWC, Bassett AS (2002) Fine mapping of the schizophrenia susceptibility locus on chromosome 1q22. Hum Hered 54:199–209.

Chazal G, Durbec P, Jankovski A, Rougon G, Cremer H. (2000). Consequences of neural cell adhesion molecule deficiency on cell migration in the rostral migratory stream of the mouse. J Neurosci. 20(4):1446-57. doi: 10.1523/JNEUROSCI.20-04-01446.2000. PMID: 10662835; PMCID: PMC6772373.

Cheung, T., Rando, T. (2013). Molecular regulation of stem cell quiescence. *Nat Rev Mol Cell Biol* **14,** 329–340. https://doi.org/10.1038/nrm3591

Conover, J. C., & Todd, K. L. (2017). Development and aging of a brain neural stem cell niche. *Experimental gerontology*, *94*, 9–13. https://doi.org/10.1016/j.exger.2016.11.007

Curtis MA, Kam M, Nannmark U, et al. (2007). Human neuroblasts migrate to the olfactory bulb via a lateral ventricular extension. Science. 315:1243–1249.

Decimo, Ilaria et al. (2012). "Neural stem cell niches in health and diseases." Current pharmaceutical design vol. 18,13: 1755-83. doi:10.2174/138161212799859611

Derkach, D., Kehtari, T., Renaud, M., Heidari, M., Lakshman, N., & Morshead, C. M. (2021). Metformin pretreatment rescues olfactory memory associated with

subependymal zone neurogenesis in a juvenile model of cranial irradiation. Cell reports. Medicine, 2(4), 100231.

Ellis P, Fagan BM, Magness ST, Hutton S, Taranova O, Hayashi S, McMahon A, Rao M, Pevny L. (2004). SOX2, a persistent marker for multipotential neural stem cells derived from embryonic stem cells, the embryo or the adult. Dev Neurosci. 26(2-4):148-65. doi: 10.1159/000082134.

Eom TY, Li J, Anton ES. (2010). Going tubular in the rostral migratory stream: neurons remodel astrocyte tubes to promote directional migration in the adult brain. Neuron. 67:173–175.

Ferreira A, Caceres A. (1992). Expression of the class III beta-tubulin isotype in developing neurons in culture. J Neurosci Res. 32(4):516-29. doi: 10.1002/jnr.490320407. PMID: 1527798.

Frazier LL, Brunjes PC. (1988). Unilateral odor deprivation: early postnatal changes in olfactory bulb cell density and number. J Comp Neurol. 269(3):355-70. doi: 10.1002/cne.902690304. PMID: 3372719.

Fukuchi-Shimogori T., Grove E.A. (2001). Neocortex patterning by the secreted signaling molecule FGF8. Science. 294:1071–74.

Furuta Y., Piston D.W., Hogan B.L. (1997). Bone morphogenetic proteins (BMPs) as regulators of dorsal forebrain development. Development. 124:2203–12.

Gao Z, Ure K, Ding P, Nashaat M, Yuan L, Ma J, Hammer RE, Hsieh J. (2011). The master negative regulator REST/NRSF controls adult neurogenesis by restraining the

neurogenic program in quiescent stem cells. J Neurosci Off J Soc Neurosci. 31(26):9772–9786. doi: 10.1523/JNEUROSCI.1604-11.2011.

Goldberg, J. S., & Hirschi, K. K. (2009). Diverse roles of the vasculature within the neural stem cell niche. Regenerative medicine, 4(6), 879–897.

Gong Q., Shipley M.T. (1995). Evidence that pioneer olfactory axons regulate telencephalon cell cycle kinetics to induce the formation of the olfactory bulb. Neuron. 14:91–101.

Gorski JA, Talley T, Qiu M, Puelles L, Rubenstein JL, Jones KR. (2002). Cortical excitatory neurons and glia, but not GABAergic neurons, are produced in the Emx1-expressing lineage. J Neurosci. 22(15):6309-14. doi: 10.1523/JNEUROSCI.22-15-06309.2002. PMID: 12151506; PMCID: PMC6758181.

Guarnieri, F. C., de Chevigny, A., Falace, A., & Cardoso, C. (2018). Disorders of neurogenesis and cortical development. *Dialogues in clinical neuroscience*, *20*(4), 255–266. https://doi.org/10.31887/DCNS.2018.20.4/ccardoso

Gunhaga L., Marklund M., Sjodal M., Hsieh J.C., Jessell T.M., Edlund T. (2003). Specification of dorsal telencephalic character by sequential Wnt and FGF signaling. Nat Neurosci. 6:701–7.

Habela, C. W., Yoon, K. J., Kim, N. S., Taga, A., Bell, K., Bergles, D. E., Maragakis, N. J., Ming, G. L., & Song, H. (2020). Persistent Cyfip1 Expression Is Required to Maintain the Adult Subventricular Zone Neurogenic Niche. *The Journal of*

neuroscience : the official journal of the Society for Neuroscience, *40*(10), 2015–2024. https://doi.org/10.1523/JNEUROSCI.2249-19.2020

Hack MA, Saghatelyan A, de Chevigny A, et al. (2005). Neuronal fate determinants of adult olfactory bulb neurogenesis. Nat Neurosci. 8:865–872.

Hardy, D., Malvaut, S., Breton-Provencher, V. *et al.* (2018). The role of calretinin-expressing granule cells in olfactory bulb functions and odor behavior. *Sci Rep* **8,** 9385. https://doi.org/10.1038/s41598-018-27692-8

Hatten ME. (1999). Central nervous system neuronal migration. *Annu Rev Neurosci.* 22:511–539.

Hébert J.M., Mishina Y., McConnell S.K. (2002). BMP signaling is required locally to pattern the dorsal telencephalic midline. Neuron. 35:1029–41.

Hevner RF, Neogi T, Englund C, Daza RA, Fink A. (2003). Cajal-Retzius cells in the mouse: transcription factors, neurotransmitters, and birthdays suggest a pallial origin. Brain Res Dev Brain Res. Mar 14;141(1-2):39-53. doi: 10.1016/s0165-3806(02)00641-7.

Hinds J. W. (1968). Autoradiographic study of histogenesis in the mouse olfactory bulb. I. Time of origin of neurons and neuroglia. *J. Comp. Neurol.* 134 287–304 10.1002/cne.901340304

Ihrie R. A., Álvarez-Buylla A. (2011). Lake-front property: a unique germinal niche by the lateral ventricles of the adult brain. *Neuron.* 70(4):674–686.

Imamura F, Greer CA. Segregated labeling of olfactory bulb projection neurons based on their birthdates. Eur J Neurosci. 2015 Jan;41(2):147-56. doi: 10.1111/ejn.12784. Epub 2014 Nov 13.

Imamura F., Ayoub A. E., Rakic P., Greer C. A. (2011). Timing of neurogenesis is a determinant of olfactory circuitry. *Nat. Neurosci.* 14 331–337 10.1038/nn.2754

Imura T, Kornblum HI, Sofroniew MV. (2003). The predominant neural stem cell isolated from postnatal and adult forebrain but not early embryonic forebrain expresses GFAP. J Neurosci. 23(7):2824-32. doi: 10.1523/JNEUROSCI.23-07-02824.2003.

Jimenez D., Garcia C., de Castro F., Chedotal A., Sotelo C., de Carlos J.A., Valverde F., Lopez Mascaraque L. (2000). Evidence for intrinsic development of olfactory structures in Pax-6 mutant mice. J Comp Neurol. 428:511–26.

Kaneko N, Marín O, Koike M, et al. (2010). New neurons clear the path of astrocytic processes for their rapid migration in the adult brain. Neuron. 67:213–223.

Kao C.F., Lee T. (2010). Birth time/order-dependent neuron type specification. *Curr. Opin. Neurobiol.* 2010;20:14–21. doi: 10.1016/j.conb.2009.10.017.

Kass, M., Czarnecki, L., Moberly, A. *et al.* (2017). Differences in peripheral sensory input to the olfactory bulb between male and female mice. *Sci Rep* **7,** 45851. https://doi.org/10.1038/srep45851

Kikuta, S., Fletcher, M. L., Homma, R., Yamasoba, T., and Nagayama, S. (2013). Odorant response properties of individual neurons in an olfactory glomerular module. *Neuron* 77, 1122–1135. doi: 10.1016/j.neuron.2013.01.022

Kim, J. Y., Choe, J., & Cheil (2020). Distinct Developmental Features of Olfactory Bulb Interneurons. *Molecules and cells*, *43*(3), 215–221. https://doi.org/10.14348/molcells.2020.0033

Lacar, B., Young, S. Z., Platel, J. C., & Bordey, A. (2011). Gap junction-mediated calcium waves define communication networks among murine postnatal neural progenitor cells. *The European journal of neuroscience*, *34*(12), 1895–1905. https://doi.org/10.1111/j.1460-9568.2011.07901.x

Lederer, C., Torrisi, A., Pantelidou, M., Santama, N., & Cavallaro, S. (2007). Pathways and genes differentially expressed in the motor cortex of patients with sporadic amyotrophic lateral sclerosis. *BMC Genomics*, 8: 26.

Lee, Ji Yeoun. (2019). "Normal and Disordered Formation of the Cerebral Cortex : Normal Embryology, Related Molecules, Types of Migration, Migration Disorders." *Journal of Korean Neurosurgical Society* vol. 62,3 (2019): 265-271. doi:10.3340/jkns.2019.0098

Li DQ, Hou YF, Wu J, Chen Y, Lu JS, Ou GH, Di ZL, Shen ZZ, Ding J, Shao ZM. (2006). Gene expression profile analysis of an isogenic tumour metastasis model reveals a functional role for oncogene AF1Q in breast cancer metastasis. *Eur J Cancer.* 42:3274–3286.

Li, W., Ji, M., Lu, F., Pang, Y., Dong, X., Zhang, J., Li, P., Ye, J., Zang, S., Ma, D., & Ji, C. (2018). Novel AF1q/*MLLT11* favorably affects imatinib resistance and cell survival in chronic myeloid leukemia. Cell death & disease, 9(9), 855.

Lin HJ, Shaffer KM, Sun Z, Jay G, He WW, Ma W. (2004). AF1q, a differentially expressed gene during neuronal differentiation, transforms HEK cells into neuron-like cells. Brain Res Mol Brain Res. 131:126–130.

Lin, R., Cai, J., Kenyon, L., Iozzo, R., Rosenwasser, R., & Iacovitti, L. (2019). Systemic Factors Trigger Vasculature Cells to Drive Notch Signaling and Neurogenesis in Neural Stem Cells in the Adult Brain. *Stem cells (Dayton, Ohio)*, *37*(3), 395–406. https://doi.org/10.1002/stem.2947

Livet J, Weissman TA, Kang H, Draft RW, Lu J, Bennis RA, Sanes JR, Lichtman JW. (2007). Transgenic strategies for combinatorial expression of fluorescent proteins in the nervous system. Nature. 450(7166):56-62. doi: 10.1038/nature06293.

Lledo PM, Merkle FT, Alvarez-Buylla A. (2008). Origin and function of olfactory bulb interneuron diversity. Trends Neurosci. 31:392–400.

Lodovichi C, Belluscio L. (2012) Odorant receptors in the formation of the olfactory bulb circuitry. Physiology (Bethesda). 27(4):200-12. doi: 10.1152/physiol.00015.2012. PMID: 22875451.

Lois C, Alvarez-Buylla A. (1994). Long-distance neuronal migration in the adult mammalian brain. Science. 264:1145–1148.

Lois C, García-Verdugo JM, Alvarez-Buylla A. (1996). Chain migration of neuronal precursors. Science. 271:978–981.

Mallamaci A., Muzio L., Chan C.H., Parnavelas J., Boncinelli E. (2000). Area identity shifts in the early cerebral cortex of Emx2S/S mutant mice. Nat Neurosci. 3:679–86.

Marin O. (2012). Interneuron dysfunction in psychiatric disorders. *Nat Rev Neurosci.*13(2):107–120.

Marins M, Xavier AL, Viana NB, Fortes FS, Fróes MM, Menezes JR. (2009). Gap junctions are involved in cell migration in the early postnatal subventricular zone. *Dev Neurobiol.* 69:715–730.

Martínez-Cerdeño, V., & Noctor, S. C. (2014). Cajal, Retzius, and Cajal-Retzius cells. Frontiers in neuroanatomy, 8, 48.

Martinez-Molina, N., Kim, Y., Hockberger, P., & Szele, F. G. (2011). Rostral migratory stream neuroblasts turn and change directions in stereotypic patterns. *Cell adhesion & migration*, *5*(1), 83–95. https://doi.org/10.4161/cam.5.1.13788

Melrose, J., Hayes, A. J., & Bix, G. (2021). The CNS/PNS Extracellular Matrix Provides Instructive Guidance Cues to Neural Cells and Neuroregulatory Proteins in Neural Development and Repair. International journal of molecular sciences, 22(11), 5583.

Merchenthaler I, Lane MV, Numan S, Dellovade TL. (2004). Distribution of estrogen receptor alpha and beta in the mouse central nervous system: in vivo autoradiographic and immunocytochemical analyses. J Comp Neurol. 473(2):270-91. doi: 10.1002/cne.20128.

Merkle F. T., Fuentealba L. C., Sanders T. A., Magno L., Kessaris N., Alvarez-Buylla A. (2014). Adult neural stem cells in distinct microdomains generate previously unknown interneuron types. *Nature Neuroscience.* 2014;**17**(2):207–214. doi: 10.1038/nn.3610.

Miragall F, Albiez P, Bartels H, de Vries U, Dermietzel R. (1997). Expression of the gap junction protein connexin43 in the subependymal layer and the rostral migratory stream of the mouse: evidence for an inverse correlation between intensity of connexin43 expression and cell proliferation activity. *Cell Tissue Res.* 1997;287:243–253.

Mirzadeh Z, Merkle FT, Soriano-Navarro M, et al. Neural stem cells confer unique pinwheel architecture to the ventricular surface in neurogenic regions of the adult brain. Cell Stem Cell. 2008;3(3):265–278.

Mirzadeh, Z., Merkle, F. T., Soriano-Navarro, M., Garcia-Verdugo, J. M., & Alvarez-Buylla, A. (2008). Neural stem cells confer unique pinwheel architecture to the ventricular surface in neurogenic regions of the adult brain. *Cell stem cell*, *3*(3), 265–278. https://doi.org/10.1016/j.stem.2008.07.004

Mizuguchi, R., Naritsuka, H., Mori, K., Mao, C. A., Klein, W. H., & Yoshihara, Y. (2012). Tbr2 deficiency in mitral and tufted cells disrupts excitatory-inhibitory balance of neural circuitry in the mouse olfactory bulb. *The Journal of neuroscience : the official journal of the Society for Neuroscience*, *32*(26), 8831–8844. https://doi.org/10.1523/JNEUROSCI.5746-11.2012

Mobley, A. S., Bryant, A. K., Richard, M. B., Brann, J. H., Firestein, S. J., & Greer, C. A. (2013). Age-dependent regional changes in the rostral migratory stream. *Neurobiology of aging*, *34*(7), 1873–1881. https://doi.org/10.1016/j.neurobiolaging.2013.01.015

Moore, S.A., and Iulianella, A. (2021). Development of the Mammalian Cortical Hem and its derivatives: the Choroid Plexus, Cajal-Retzius Cells, and Hippocampus. *Open Biology*. doi.org/10.1098/rsob.210042

Mori K, Sakano H. (2011). How is the olfactory map formed and interpreted in the mammalian brain? Annu Rev Neurosci. 34:467-99. doi: 10.1146/annurev-neuro-112210-112917.

Mullen RJ, Buck CR, Smith AM. (1992). NeuN, a neuronal specific nuclear protein in vertebrates. Development. 116(1):201-11. doi: 10.1242/dev.116.1.201.

Murata K., Imai M., Nakanishi S., et al. (2011). Compensation of depleted neuronal subsets by new neurons in a local area of the adult olfactory bulb. *Journal of Neuroscience.* **31**(29):10540–10557. doi: 10.1523/jneurosci.1285-11.2011.

Nagayama S, Homma R, Imamura F. (2014) Neuronal organization of olfactory bulb circuits. Front Neural Circuits. 8:98. doi: 10.3389/fncir.2014.00098.

Nam SC, Kim Y, Dryanovski D, et al. (2007). Dynamic features of postnatal subventricular zone cell motility: a two-photon time-lapse study. J Comp Neurol. 505:190–208.

Nam SC, Kim Y, Dryanovski D, Walker A, Goings G, Woolfrey K, Kang SS, Chu C, Chenn A, Erdelyi F, Szabo G, Hockberger P, Szele FG. (2007). Dynamic features of postnatal subventricular zone cell motility: a two-photon time-lapse study. J Comp Neurol505(2):190-208. doi: 10.1002/cne.21473.

Nishizumi, H., Miyashita, A., Inoue, N. *et al.* (2019). Primary dendrites of mitral cells synapse unto neighboring glomeruli independent of their odorant receptor identity. *Commun Biol* **2,** 14. https://doi.org/10.1038/s42003-018-0252-y

Obernier, K., Cebrian-Silla, A., Thomson, M., Parraguez, J. I., Anderson, R., Guinto, C., Rodas Rodriguez, J., Garcia-Verdugo, J. M., & Alvarez-Buylla, A. (2018). Adult Neurogenesis Is Sustained by Symmetric Self-Renewal and Differentiation. *Cell stem cell*, *22*(2), 221–234.e8. https://doi.org/10.1016/j.stem.2018.01.003

Oliveira-Pinto AV, Santos RM, Coutinho RA, Oliveira LM, Santos GB, Alho AT, Leite RE, Farfel JM, Suemoto CK, Grinberg LT, Pasqualucci CA, Jacob-Filho W, Lent R. (2014). Sexual dimorphism in the human olfactory bulb: females have more neurons and glial cells than males. PLoS One. 9(11):e111733. doi: 10.1371/journal.pone.0111733.

Osterhout J.A., El-Danaf R.N., Nguyen P.L., Huberman A.D. (2014). Birthdate and outgrowth timing predict cellular mechanisms of axon target matching in the developing visual pathway. *Cell Rep.* 8:1006–1017. doi: 10.1016/j.celrep.2014.06.063.

P. Le Baccon, D. Leroux, C. Dascalescu, S. Duley, D. Marais, E. Esmenjaud, J.J. Sotto, M. Callanan. (2001). Novel evidence of a role for chromosome 1 pericentric

heterochromatin in the pathogenesis of B-cell lymphoma and multiple myeloma. Genes Chromosom. Cancer, 32; 250-264

Padmanabhan K., Urban N. N. (2010). Intrinsic biophysical diversity decorrelates neuronal firing while increasing information content. *Nat. Neurosci.* 13 1276–1282 10.1038/nn.2630

Paez-Gonzalez P, Abdi K, Luciano D et al. (2011). Ank3-dependent SVZ niche assembly is required for the continued production of new neurons. *Neuron* 71:61–75.

Panzanelli, P., Fritschy, J. M., Yanagawa, Y., Obata, K., and Sassoe-Pognetto, M. (2007). GABAergic phenotype of periglomerular cells in the rodent olfactory bulb. *J. Comp. Neurol.* 502, 990–1002. doi: 10.1002/cne.21356

Parrish-Aungst, S., Shipley, M. T., Erdelyi, F., Szabo, G., and Puche, A. C. (2007). Quantitative analysis of neuronal diversity in the mouse olfactory bulb. *J. Comp. Neurol.* 501, 825–836. doi: 10.1002/cne.21205

Pencea V, Luskin MB. (2003). Prenatal development of the rodent rostral migratory stream. J Comp Neurol. 463:402–418.

Platel, J. C., & Bordey, A. (2016). The multifaceted subventricular zone astrocyte: From a metabolic and pro-neurogenic role to acting as a neural stem cell. Neuroscience, 323, 20–28.

Raponi E, Agenes F, Delphin C, Assard N, Baudier J, Legraverend C, Deloulme JC. (2007). S100B expression defines a state in which GFAP-expressing cells lose their

neural stem cell potential and acquire a more mature developmental stage. Glia. 55(2):165-77. doi: 10.1002/glia.20445.

Rubenstein J.L., Anderson S., Shi L., Miyashita-Lin E., Bulfone A., Hevner R. (1999). Genetic control of cortical regionalization and connectivity. Cereb Cortex. 9:524–32.

Sakano H. (2010). Neural map formation in the mouse olfactory system. Neuron. 67(4):530-42. doi: 10.1016/j.neuron.2010.07.003.

Silva-Vargas V, Maldonado-Soto AR, Mizrak D, Codega P, Doetsch F. (2016). Age-Dependent Niche Signals from the Choroid Plexus Regulate Adult Neural Stem Cells. Cell Stem Cell. 19(5):643-652. doi: 10.1016/j.stem.2016.06.013.

Simpson, K.L. & Sweazey, R.D.. (2013). Olfaction and Taste. Fundamental Neuroscience for Basic and Clinical Applications. Volume null (23): 313-323.e1. 10.1016/B978-1-4377-0294-1.00023-5.

Stanton-Turcotte, D., Hsu, K., Moore, S.A., Yamada, M., and Iulianella, A. (2022). *Mllt11* regulates the migration and neurite outgrowth of cortical projection neurons during development. *Journal of Neuroscience.* 42 (19): 3931-3948

Su YS, Ding WH, Xing MJ, Qi DK, Li ZZ, Cui DH (2017) The interaction of TXNIP and AFq1 genes increases the susceptibility of schizophrenia. Mol Neurobiol 54:4806–4812.

Tan, J., Savigner, A., Ma, M., and Luo, M. (2010). Odor information processing by the olfactory bulb analyzed in gene-targeted mice. *Neuron* 65, 912–926. doi: 10.1016/j.neuron.2010.02.011

Tiberio, P., Lozneanu, L., Angeloni, V., Cavadini, E., Pinciroli, P., Callari, M., Carcangiu, M. L., Lorusso, D., Raspagliesi, F., Pala, V., Daidone, M. G., & Appierto, V. (2017). Involvement of AF1q/*MLLT11* in the progression of ovarian cancer. Oncotarget, 8(14), 23246–23264.

Tse, W., Zhu, W., Chen, H., & Cohen, A. (1995). A novel gene, AF1q, fused to MLL in t(1;11) (q21;q23), is specifically expressed in leukemic and immature hematopoietic cells. *Blood*, 85(3):650-6.

Urbán N, Blomfield IM, Guillemot F. (2019). Quiescence of Adult Mammalian Neural Stem Cells: A Highly Regulated Rest. Neuron. 104(5):834-848. doi: 10.1016/j.neuron.2019.09.026.

Weiler E, Farbman AI. (1999). Mitral cell loss following lateral olfactory tract transection increases proliferation density in rat olfactory epithelium. Eur J Neurosci. (9):3265-75. doi: 10.1046/j.1460-9568.1999.00748.x.

Whitman MC, Greer CA. (2007). Synaptic integration of adult-generated olfactory bulb granule cells: basal axodendritic centrifugal input precedes apical dendrodendritic local circuits. J Neurosci. 27(37):9951-61. doi: 10.1523/JNEUROSCI.1633-07.2007.

Wilson RI, Mainen ZF. 2006. Early events in olfactory processing. Annu Rev Neurosci. 29:163-201. doi: 10.1146/annurev.neuro.29.051605.112950.

Yamada, M., Clark, J., & Iulianella, A. (2014). MLLT11*MLLT11*/AF1q is differentially expressed in maturing neurons during development. *Gene Expression Patterns* , 15(2): 80-87.

Yamashita T, Ninomiya M, Hernández Acosta P, et al. (2006). Subventricular zone-derived neuroblasts migrate and differentiate into mature neurons in the post-stroke adult striatum. *J Neurosci,* 26:6627–6636.

Yamashita T, Ninomiya M, Hernández Acosta P, et al. Subventricular zone-derived neuroblasts migrate and differentiate into mature neurons in the post-stroke adult striatum. J Neurosci. 2006. 26:6627–6636.

Zerlin M, Levison SW, Goldman JE. (1995). Early patterns of migration, morphogenesis, and intermediate filament expression of subventricular zone cells in the postnatal rat forebrain. J Neurosci.15(11):7238-49. doi: 10.1523/JNEUROSCI.15-11-07238.1995.

Zigova T, Pencea V, Betarbet R, et al. (1998). Neuronal progenitor cells of the neonatal subventricular zone differentiate and disperse following transplantation into the adult rat striatum. Cell Transplant. 1998. 7:137–156.

Zigova T, Pencea V, Betarbet R, et al. Neuronal progenitor cells of the neonatal subventricular zone differentiate and disperse following transplantation into the adult rat striatum. *Cell Transplant.* 1998;7:137–156